LITERATURE REVIEW OF CRITICAL BED-SHEAR STRESSES FOR MUD-SAND MIXTURES

by Leo C. van Rijn; www.leovanrijn-sediment.com

Contents

1. Approach of Shields for cohesionless sediment

1.1 Sand

The most simple approach considering initiation of motion is the flow over a perfect sphere resting on a bed of the same (uniform) particles, see **Figure 1.1**.
The forces acting on the particle are:

F_D = drag force due to fluid flow near the sand grain= $0.5\ \rho\ (0.25\ \pi\ d^2)\ C_D\ U_f^2 = \alpha_F\ \rho\ d^2\ U_f^2$

F_L = lift force due to vertical flow = $0.5\ \rho\ (0.25\ \pi\ d^2)\ C_D\ V_s^2 = \alpha_F\ \rho\ d^2\ V_s^2$

G = submerged particle weight = $\alpha_G\ (\rho_s-\rho)\ g\ d^3$

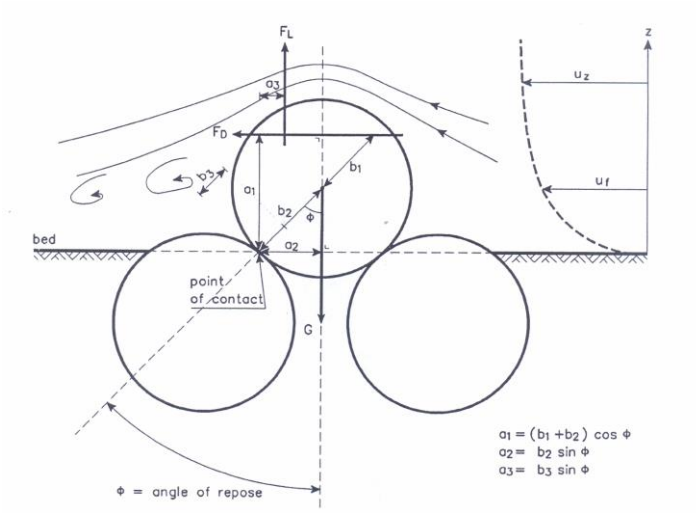

Figure 1.1 *Forces acting on sediment particle*

The particle will move around the pivot point of contact, if the moments due to the driving forces are larger than the moment due to the resisting force of gravity.
This gives: $F_D\ a_1 + F_L\ a_3 \geq G\ a_2$
Using: $a_3 = \alpha_3\ a_1$, yields: $F_D\ a_1 + F_L\ \alpha_3\ a_1 \geq G\ a_2$ or $F_D + \alpha_3\ F_L \geq (a_2/a_1)\ G$
Using: $a_1 = (b_1+b_2)\ \cos\phi$, $a_2 = b_2\ \sin\phi$, ϕ= angle of repose, it follows that:

$$\frac{F_D + \alpha_3 F_L}{G} \geq [b_2/(b_1+b_2)]\ \tan\phi \qquad (1.1)$$

$$\frac{U_f^2 + \alpha_3 V_s^2}{(s-1)\ g\ d} \geq [b_2/(b_1+b_2)]\ [\alpha_G/\alpha_F]\ \tan\phi \qquad (1.2)$$

with:

d = particle diameter,
U_f = fluid velocity at particle level,
V_s = upward flow at particle level,
ρ_s = sediment density,
ρ = fluid density,

s = (ρ_s/ρ = relative density,
C_D = drag coefficient,
α_F = 0.125 π C_D = coefficient,
α_G = α_p $\pi/6$ = coefficient.
α_3 = coefficient between 0.5 and 1,
α_p = particle shape coefficient ($\cong$1).

If $U_f >> V_s$ and $\alpha_3 \cong$ 0.5 to 1, it follows that:

$$\frac{U_f^2}{(s-1)\, g\, d} \geq [b_2/(b_1+b_2)]\, [\alpha_G/\alpha_F]\, \tan\phi \qquad (1.3)$$

The horizontal fluid flow velocity at critical conditions can be described by $U_{f,cr} = \alpha_* U_{*,cr}$.
with: $U_{*,cr} = [\tau_{b,cr}/\rho]^{0.5}$ and $\tau_{b,cr}$ = bed-shear stress at critical conditions, α_*= coefficient between 5 and 10.
This yields:

$$\theta_{cr} = \frac{U_{*,cr}^2}{(s-1)\, g\, d} \geq [b_3/(b_1+b_2)]\, [\alpha_G/\alpha_F]\, [\alpha_*]^{-1} \tan\phi \qquad (1.4)$$

Equation (1.4) is known as the Shields' equation, The right hand side of Equation (1.4) has been determined by performing experiments in flumes. The Shields' value θ_{cr} was found to be dependent on the Reynolds' number $Re_* = U_{*,cr} d/\nu$. The flow near the particle is laminar for $U_{*,cr} d/\nu < 5$. The overall flow is turbulent $Re = uh/\nu > 1000$ to 2000, with u= depth-mean flow velocity and h= water depth.

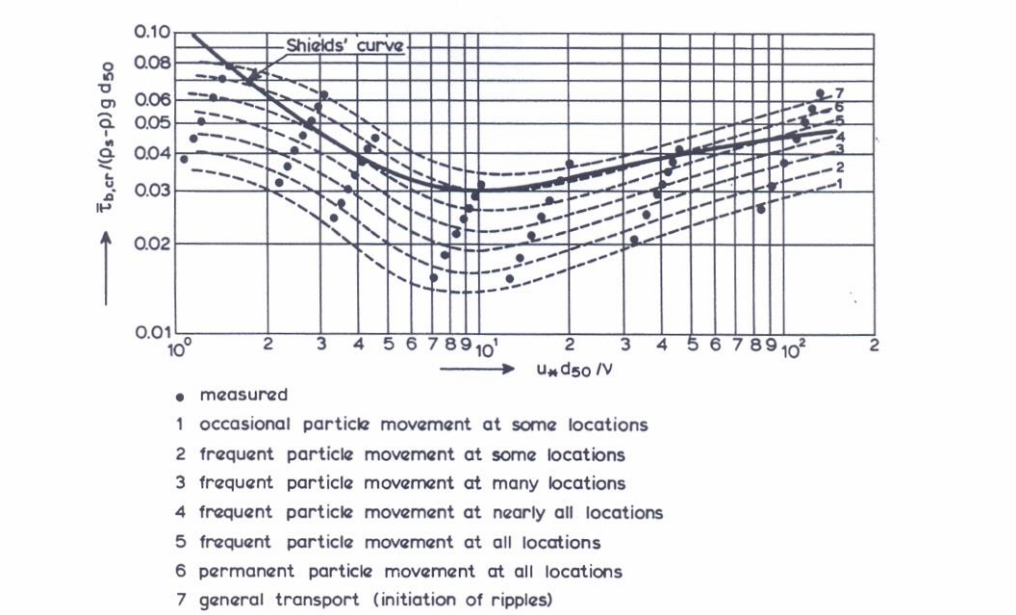

Figure 1.2 *Shields' curve as function of boundary Reynolds' number*

Figure 1.2 shows the Shields' curve as function of the Reynolds' number. Various transport stages based on visual observations in the turbulent regime are also shown. In the turbulent regime, the Shields' curve represents conditions with frequent particle movement at all locations. The 'stage' curves in the laminar

regime (left side of the plot; $Re_* < 5$) may not be very accurate; most likely the curves should gradually merge into one single curve or a narrow bundle of curves in the laminar regime.

The Shields' curve can also be shown as function of a dimensionless particle size $D_* = d[(s-1)g/\nu^2]^{1/3}$, see **Figure 1.3**.

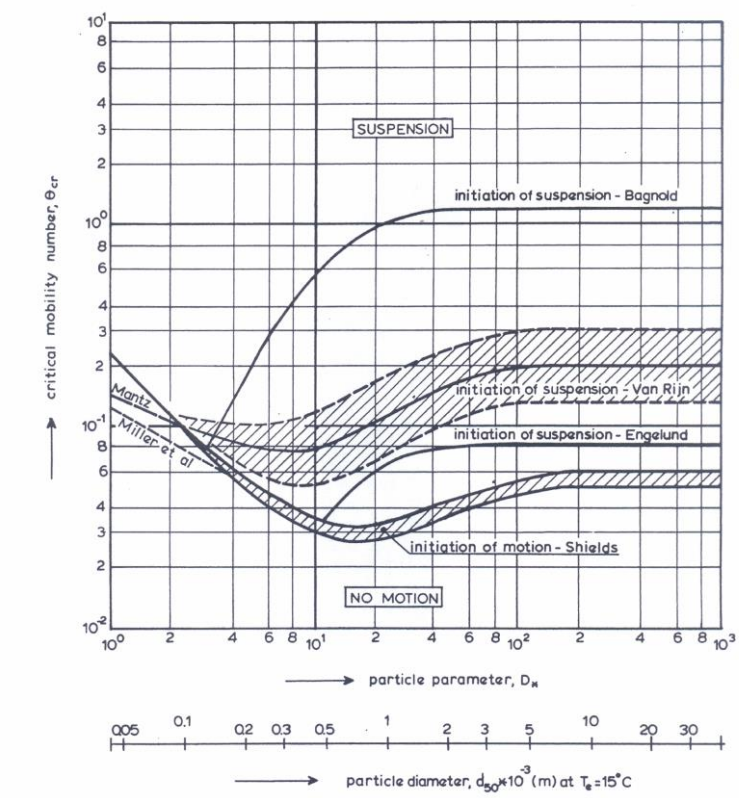

Figure 1.3 *Shields' curve as function of dimensionless particle size D_**

Initiation of motion in combined steady and oscillatory flow (wave motion) can also be expressed in terms of the Shields-parameter provided that the wave period averaged bed–shear stress is used (**Van Rijn, 1993**). Initiation of motion of widely sorted sand mixtures has been studied by Egiazaroff (1965).

Van Rijn (1993) also included the critical stress for initiation of suspension based on observations of suspended sediments in flume experiments.

Analysis of experimental work focussing on fine cohesionless sand and silt particles has shown that the original Shields-curve is not very accurate for fine sand beds (particles<0.1 mm). In the case of fine sediment, the flow may be in the laminar (viscous) rather than in the turbulent flow regime. Results of experimental work in laminar flows are discussed hereafter.

Mantz (1977) has studied incipient motion and transport of fine cohesionless (rounded) sediment grains with sizes in the range of 15 to 66 μm (D_* in the range of 0.4 to 1.7) in a long, open flume (length of 10 m) with water. The sediment bed was laid by natural deposition of grains from the recirculating water of the flume. The flow was turbulent (Re> 4000). The flow near the particles was laminar (boundary Reynolds' number $Re_* < 1$). His four test results are shown in **Figure 1.4**. The critical stage was defined as: ' the flow rate was increased until a bed load transport was visually observed'.

Mantz (1977) has also analyzed various data of White (1970) related to fully laminar flow (fine cohesionless particles of 25 to 133 μm in an oil flow). The data are shown in **Figure 1.4**.

Miller et al. (1977) have analyzed many test results of initiation of motion of very fine sediment in the range of 15 to 200 μm (in water and oil with turbulent and laminar flow). Their results cover critical Shields' values in the range of $\theta_{cr} \cong 0.051$ to 0.15, see **Figure 1.4**.

Govers (1987) has performed small-scale flume experiments (length= 1.5 m, width= 0.06 m) on incipient motion in laminar and turbulent flow conditions (water). The sediment bed extended over the length of the flume. The flow depth was about 5 mm for laminar flow and about 10 mm for turbulent flow. Six sediment samples have been tested: 0.045, 0.127, 0.218, 0.414, 0.661 and 1.098 mm. He found a significant larger critical shear stress for laminar flow than for turbulent flow using the same sediment. The results are shown in **Figure 1.4**. Govers has observed that the movement of grains in laminar flow happens in a different way than in turbulent flow. Once a grain is detached it keeps moving at a nearly constant velocity and brings other grains into motion so that a moving grain carpet is formed.

Pilotti and Menduni (2001) have studied the initiation of motion of sediment particles in viscous flows (water and water-glucose solutions) at low boundary Reynolds' numbers (Re_*) in the range of 0.01 to 10. Sediment grains were only present in a small section (patch) of the flume with length of 0.175 m and width of 0.05 m. The flume bottom was smooth and plane. The critical stage was defined as: 'inception of transport is a progressive mobilisation of a substantial percentage of grains followed by a collapse of the bed surface'. Their experimental results are given by the following ranges:

Re_*= 0.1 $\rightarrow$ θ_{cr}= 0.12 to 0.25
Re_*= 1 $\rightarrow$ θ_{cr}= 0.1 to 0.2
Re_*= 10 $\rightarrow$ θ_{cr}= 0.06 to 0.12

The scatter of the results is relatively large, which may be caused by the rather small water depths used (about 1.5 mm) and the transition in roughness from the smooth flume bottom to the small sediment surface. Therefore, these results may be less reliable (not shown in Figure 1.4).

Loiseleux et al. (2005) have studied the onset of erosion of spherical glass beads with diameters in the range of 0.1 to 0.22 mm in a small tilting flume-type apparatus (length of about 1.3 m). The sediment bed also had a length of about 1.3 m. The flow was in the laminar regime. The onset of erosion was defined as the lowest flow rate for which grains are still being eroded after 15 minutes and after some times a ripple pattern develops. The results (4 data points) for a horizontal bed are given in **Figure 1.4**.

Figure 1.4 shows the experimental data of White (1940), White (1970), Ward 1967, Mantz 1977, Miller et al. 1977, Govers 1987, Yalin-Karahan 1979 and Loiseleux et al. 2005 as function of the dimensionless D_* parameter. The experimental range of Shields (1936) for coarser sediments is also shown. The scatter of the experimental results in the rangre $1<D_*<10$ is somewhat larger than that of the Shields' curve. The scatter for $D_*<1$ is considerable, which is an inherent effect of testing very small sediments (less visible, plane bed is less well defined due to additional small irregularities on bed surface, etc.).
The upper envelope of the experimental range in the laminar regime can be seen as: general bed load transport with grains moving at all locations (collapse of the bed surface and initiation of ripple patterns).
The lower envelope (about 30% lower) of the experimental range in the laminar regime can be seen as: frequent particle movement at nearly all locations.

For $D_* < 1$ the critical Shields' values for fully laminar flow (Re < 1000) are within the same range as those for turbulent flow (Re > 1000).
For $D_* \geq 1$ the critical Shields values for fully laminar flow are larger than those for turbulent flow.

The data for both laminar and turbulent flows can be represented by Equations 1.5 and 1.6.

The critical shear stress for initiation of motion and suspension in laminar and turbulent flows can be represented by the following general curves (see tool: **sedimentparameters.xls**):

$$\theta_{cr,motion} = 0.3/(1+D_*) + 0.055\,[1-\exp(-0.02D_*)] \quad \text{for } D_* > 0.1 \qquad (1.5)$$

$$\theta_{cr,suspension} = 0.3/(1+D_*) + 0.1\,[1-\exp(-0.05D_*)] \quad \text{for } D_* > 0.1 \qquad (1.6)$$

with:

D_* = $d_{50}\,[(s-1)\,g/\nu^2]^{1/3}$= dimensionless grain size,
θ_{cr} = $\tau_{b,cr}/[(\rho_s-\rho)gd_{50}]$= dimensionless critical shear stress,
$\tau_{b,cr}$ = $\rho\, g\, U_{cr}^2/C^2$ = bed-shear stress,
C = $5.75\, g^{0.5}\, \log(12h/(3d_{90}))$,
s = ρ_s/ρ= relative density,
ρ_s = sediment density (2650 kg/m^3),
ρ = fluid density (kg/m^3),
ν = kinematic viscosity coefficient (=0.000001 m^2/s),
g = acceleration of gravity (9.81 m/s^2),
d_{90} =$2d_{50}$ = particle size.

Both Equations (1.5 and 1.6) are shown in **Figure 1.4.**

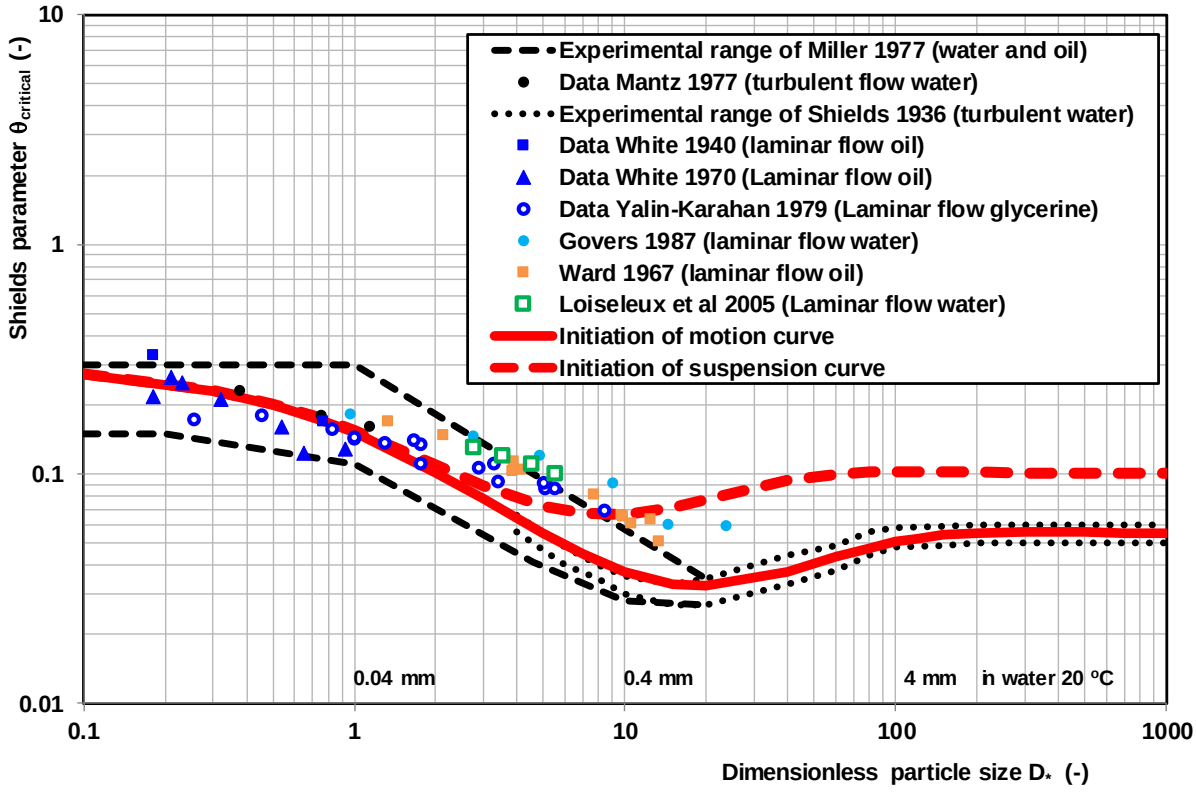

Figure 1.4 *General Shields diagram for laminar and turbulent flows*

Figure 1.5 shows the critical bed-shear stress for initiation of motion ($\tau_{cr,motion}$) and suspension ($\tau_{cr,suspension}$) given a water temperature of 15° Celsius (viscosity effect). The critical bed-shear stress decreases systematically for decreasing particle sizes. The critical bed-shaer stress for fine (clay-silt type) particles smaller than 10 μm are < 0.05 N/m^2 (neglecting cohesion).

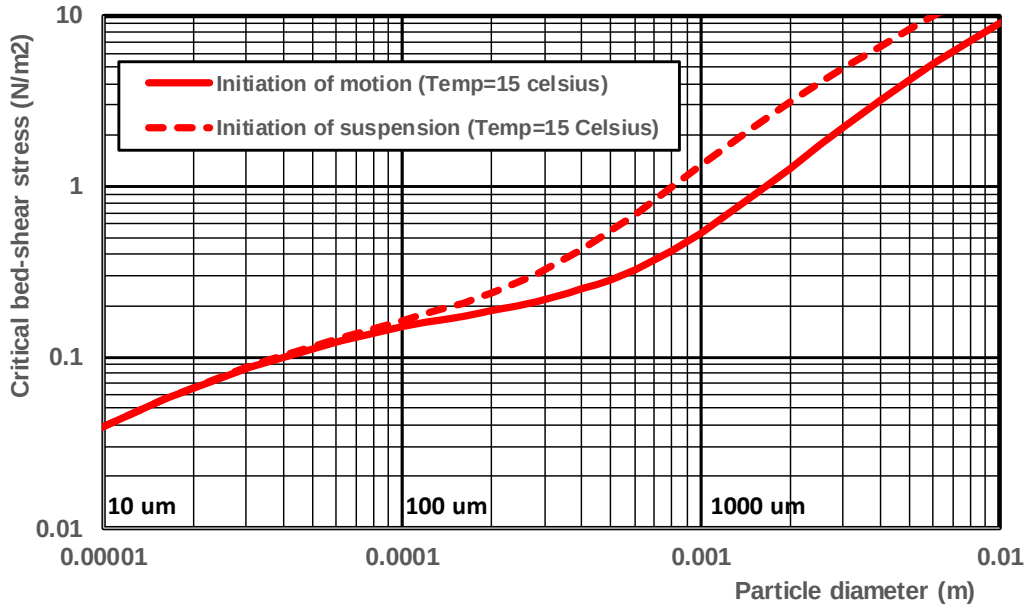

Figure 1.5 *Critical bed-shear stress for initiation of motion and suspension*

Figure 1.6 shows the critical depth-averaged flow velocity for initiation of motion ($U_{cr,motion}$) and suspension ($U_{cr,suspension}$) for water depths between 1 and 20 m. The depth-avergaged critical flow velocity for fine sediments of 10 to 20 μm are about 0.2 m/s in water depth of about 1 m.

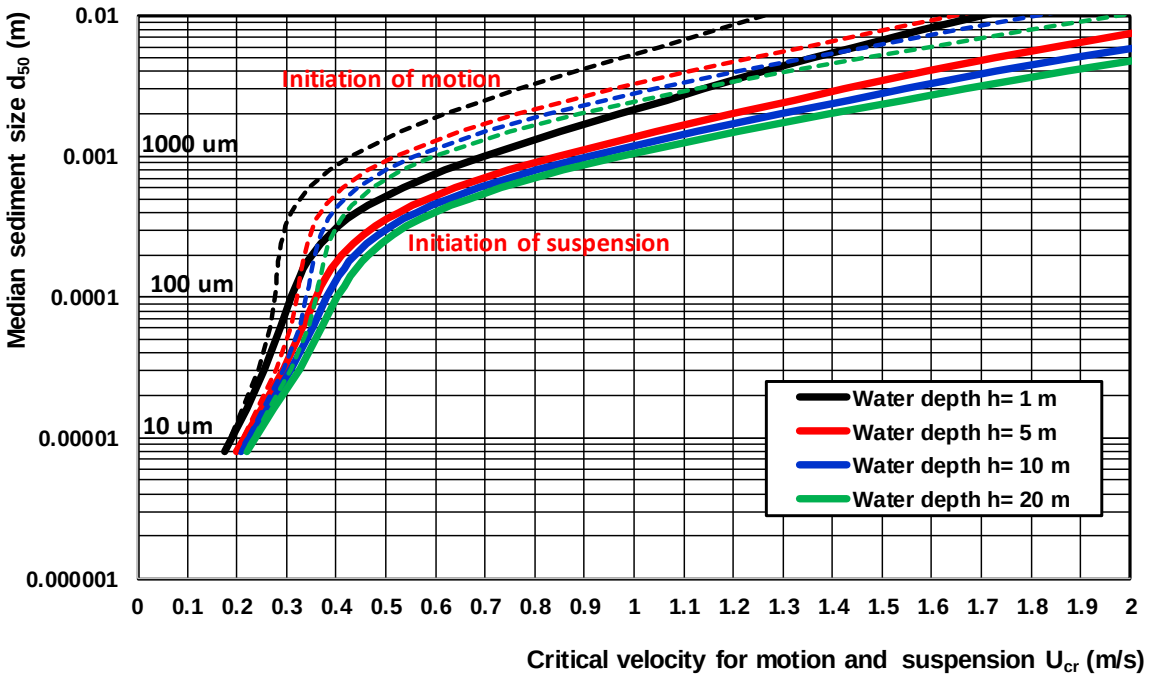

Figure 1.6 *Critical depth-averaged velocity for initiation of motion and suspension*

1.2 Shells

Calcareous shells in convex upward position (hollow side to the sediment surface, see **Figure 1.7**) can be used to stabilize sand beaches against erosion. The onset of motion of the shells can be derived from the Shields equation. Dey (2003) has done experimental work on incipient motion of bivalve shells. A shell is represented by a grain with an effective diameter (d_{eff}) of the same height as the shell height, see **Figure 1.7**.

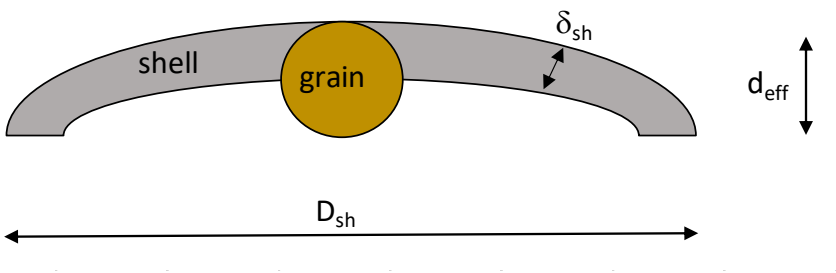

Figure 1.7 *Definition sketch of a shell normal to the flow (convex upward position)*

The shell thickness is defined as: $\delta_{sh} = \alpha_1 D_{sh}$ with α_1= 0.03-0.05.
The shell height is defined as: $d_{eff} = \alpha_2 D_{sh}$ with α_2= 0.2-0.3.
D_{sh}= length of shell
The drag coefficients in the case of flow normal to the objects are given by: $C_{D,shell}$= 0.1 and $C_{D,grain}$=0.5.
The Shields-parameter is defined as (see Equation 1.1) : $\theta = F_D/G = [0.5\ \rho\ C_D\ A_{normal}\ U_f^2]/[(\rho_s-\rho)\ g\ V]$
with: A_{normal}= area of object normal to the flow direction, U=velocity; V= volume of object, as follows:
$A_{shell} = \alpha_3\ d_{eff}\ D_{sh}$ with α_3= 0.5 - 0.7 and $V_{shell} = 0.25\ \pi\ D_{sh}^2\ \delta_{sh} = 0.25\ \alpha_1\ \pi\ D_{sh}^3$
$A_{grain} = 0.25\ \pi\ (d_{eff})^2$ and $V_{grain} = (1/6)\ \pi\ (d_{eff})^3$
The Shields-parameters are:

θ_{shell} $= [0.5\ \rho\ C_{D,shell}\ \alpha_3\ d_{eff}\ D_{sh}\ U_{f,shell}^2]/[(\rho_s-\rho)\ g\ 0.25\ \alpha_1\ \pi\ D_{sh}^3]$
$= [0.5\ \rho\ C_{D,shell}\ \alpha_3\ d_{eff}\ U_{f,shell}^2]/[(\rho_s-\rho)\ g\ 0.25\ \alpha_1\ \pi\ D_{sh}^2] = [0.6\ \alpha_3 C_{D,shell}\ d_{eff}\ U_{f,shell}^2]/[\ \alpha_1\ (s-1)\ g\ D_{sh}^2]$
$= [0.6\ \alpha_3 C_{D,shell}\ \alpha_2\ D_{sh}\ U_{f,shell}^2]/[\ \alpha_1\ (s-1)\ g\ D_{sh}^2] = [0.6\ \alpha_2\alpha_3 C_{D,shell}\ U_{f,shell}^2]/[\ \alpha_1\ (s-1)\ g\ D_{sh}]$

θ_{grain} $= [0.5\ \rho\ C_{D,grain}\ 0.25\ \pi\ (d_{eff})^2\ U_{f,grain}^2]/[(\rho_s-\rho)\ g\ 0.166\ \pi\ d_{eff}^3]$
$= [0.75\ C_{D,grain}\ U_{f,grain}^2]/[(s-1)\ g\ d_{eff}]$

Assuming that the specific density of shell is about 2600 kg/m^3 (similar to that of sand), it follows that:
$\theta_{shell}/\theta_{grain} = 0.8\ \{(\alpha_2)^2\ \alpha_3/\alpha_1\}\ (C_{D,shell}/C_{D,grain})\ (U_{f,shell}/U_{f,grain})^2$
Using: $(C_{D,shell}/C_{D,grain})$ = 0.2; $U_{f,shell}/U_{f,grain}$= 1.1 (larger velocities for shells lying on fine sand bed); α_1= 0.03-0.05, α_2= 0.25, α_3=0.6, it follows that: $\theta_{shell}/\theta_{grain}$ = 0.1 - 0.3. Thus, the mobility of a flat shell is much lower than that of an equivalent sand grain of the same height. **Table 1.1** shows examples of computed θ-values for shells. Shells are stabile for θ<0.05.
Miedema and Ramsdell (2011) report critical shear stress values for small shells in the range of 0.4 to 0.7 N/m^2 (equivalent to that of sand grains of 1 to 1.5 mm) but much larger than that of a fine sand grain of 0.2 to 0.3 mm (0.2-0.3 N/m^2). Hence, small shells protect a fine sand bed against erosion.
A small shell may have a critical shear stress of about 0.5 N/m^2 (same as coarse sand).
A large shell may have a critical shear stress of about 1 to 2 N/m^2 (same as gravel).

Type of shell	**d_{eff} (mm)**	**U_f (m/s)**	**θ_{shell} (-)**
D_{shell}= 30 mm; δ_{shell}= 1.5 mm (α_1=0.04; α_3=0.6; C_d=0.1)	6 (α_2= 0.2)	0.1 0.3	0.004 0.035
D_{shell}= 60 mm; δ_{shell}= 2 mm (α_1=0.033; α_3=0.6; C_d=0.1)	15 (α_2= 0.25)	0.1 0.4	0.002 0.03

Table 1.1 *Examples of mobility parameter of shells*

2. Sediment mixtures with cohesive properties (mud-sand mixtures)

2.1 Sediment mixture definitions

The grain size scale of the American Geophysical Union for sediments with particle sizes smaller than 2 mm consists of about 13 subclasses ranging from very coarse sand to very fine clay. Herein, five somewhat broader subclasses are distinguished:

coarse sand (non-cohesive)	0.5 to 2 mm	(500 to 2000 μm)
fine sand (non-cohesive)	0.063 to 0.5 mm	(63 to 500 μm)
coarse silt (sometimes cohesive)	0.032 to 0.063 mm	(32 to 63 μm)
fine silt (weakly cohesive)	0.08 to 0.32 mm	(8 to 32 μm)
clay+very fine silt (very cohesive)	<0.08 mm	(< 8 μm)

The following class separation diameters are herein used: d_{gravel}=2000 μm, d_{sand}=63 μm, d_{silt}=32 μm, d_{fine}= 8 μm. Basically, the pure clay fraction is the fraction with sediments smaller than 2 μm (lutum). For practical reasons (laboratory determination of the percentage<2 μm is extremely difficult), the cohesive fraction with clay and very fine silt is herein defined to consist of particles with diameters smaller than 8 μm (clay-dominated fraction). Bed samples consisting of mixtures of clay, silt and sand are herein classified as: mud, sandy mud, silty mud or clayey mud, depending on the percentages of sand, silt, clay and organic material (**Table 2.1**). Mud is defined as the sediment mixture/fraction with particles smaller than 63 μm.

Type of sediment		Percentage of organic material	Percentage of Clay+Fine Silt (< 8 μm)	Percentage of Silt (8 to 63 μm)	Percentage of Sand (> 63 μm)
Sand	(non-cohesive)	0%	0%	0%	100%
Muddy Sand	(weakly-cohesive)	0-10%	0-5%	20-40%	60-80%
Sandy Mud	(cohesive)	0-10%	5-10%	30-60%	60-30%
Mud	(cohesive)	0-20%	10-20%	50-70%	0-10%
Silty Mud	(cohesive)	0-20%	10-40%	60-80%	0%
Clayey Mud	(cohesive)	0-20%	40-60%	40-60%	0%

Table 2.1 *Types of sand-mud mixtures*

Layered beds

Bed deposits formed in sedimentary environments often have layered structures due to differential settling and sediment sorting. Each layer may have a different structure, bulk density (degree of consolidation) and strength against erosion resulting in a stepwise erosional behaviour. Generally, the topmost layer is a thin muddy layer as the very fine particles will settle at the end of the settling process. The upper muddy layer generally has a low strength against erosion (about 0.1 N/m^2), if it is a freshly deposited layer and the mud particles will almost immediately be suspended, when the flow-induced bed-shear stress exceeds the critical shear stress. A sandy sub-layer underneath a thin mud layer will be eroded as bed load transport with ripple features occurring. Other more consolidated mud layers underneath sand layers may have a much higher erosion strength due to consolidation processes.

Mixed beds

Homogeneously mixed sediment beds of clay, slit and sand particles are rare in nature. A typical example of a rather homogeneously mixed bed is the bed surface of an intertidal flat exposed to waves due to the active reworking of the bed surface by the surface waves.

Homogeneously mixed beds have often been used in laboratory experiments. These types of laboratory mixtures generally are somewhat bimodal by mixing fine sand and natural mud with low silt contents. The presence of sand improves the drainage, resulting in more compaction. Consolidation increases with increasing percentage of sand. The sediment properties are approximately constant over the depth of the layer.
The results of laboratory experiments show that there is an optimal ratio of sand-mud content at which the critical erosion shear stress of the sand-mud particles is maximum. The optimum mud content appears to be between 30% and 40% by weight. In that case, the sand particles are completely coated by the mud particles resulting in an increase of the erosion strength of the sand particles. Furthermore, the bulk density is affected for a mud content > 30%. Depending on the compaction time scale, the dry bulk density may vary in the range of 400 to 1200 kg/m^3. Laboratory observations have shown that the pick-up process of the sand particles is slowed down by the presence of the clay-silt particles. The clay-silt particles are washed out together with the sand particles. The critical shear stress of the sand fraction is dependent on the mineralogy and grain size of the mud and sand fractions (Mitchener and Torfs, 1996).

Network structure

In tidal rivers (estuaries) the bed generally consists of a mixture of sand, silt, clay and organic materials. The sand, silt and clay mixture generally behaves as a mixture with cohesive properties when the clay-silt fraction (<63 μm) is larger than about 0.3 and as a non-cohesive mixture when the mud fraction is smaller than about 0.3. The distinction between non-cohesive mixtures and cohesive mixtures can be related to a critical clay-silt or mud content ($p_{mud,cr}$).

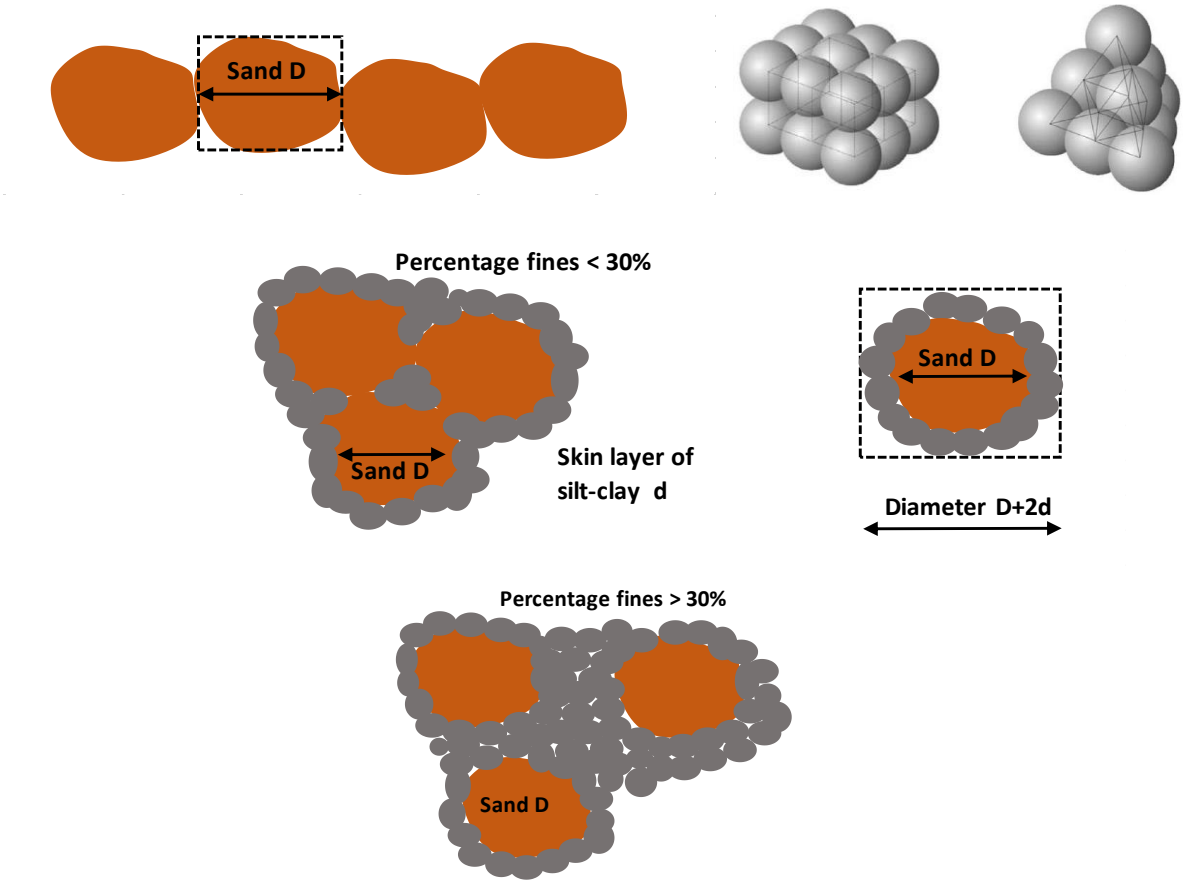

Figure 2.1 *Network structures of mud-sand mixtures*
Upper: sand particles withoud mud
Middle: sand particles with skin layer of silt-clay particles (percentage fines < 30%)
Lower: sand particles drowned in mud particles (percentage fines > 30%)

True cohesion is a soil property mainly depending on electro-chemical bonds between the particles, often enhanced by organic polymers in the soil. Cohesive effects in mud-sand mixtures become important in the case that the sand particles are fully surrounded (coated) by fine cohesive particles.
A mixture of sand particles (diameter D) can form a network structure, if each sand particle is in a cube with diameter D and all cubes are closely packed creating a network structure with contact between all sand particles, see **Figure 2.1 (upper)**. The volume concentration c_{sand} can be defined as the ratio of the sand particle volume ($0.16\pi D^3$ for a sphere) and the cube volume (D^3) resulting in $c_{sand} \cong 0.5$ (volume concentration). Thus, all sand particles are in contact for a volume concentration of about 0.5. This packing arrangement is known as cube-packing. A stronger network is obtained for a hexagonal-packing resulting in a volume concentration of about 0.7, see **Figure 2.1 (upper)**.
If one sand particle with diameter D is surrounded by a layer of fine particles with diameter d, the total volume of the fine particles in the skin layer is about: $V_{fines} = (1-\varepsilon)\ 1.33\pi\ [(0.5D+d)^3-(0.5D)^3]$ with ε= pore volume of the fine particles (about 0.4).
The cube around a sand particle (diameter D) plus the skin layer of fine particles (diameter d) has a volume of $V_{cube,sand+fines}=(D+2d)^3$.
The volume concentration of fine particles is: $c_{fines}=V_{fines}/V_{cube,sand+fines}= (1-\varepsilon)1.33\pi[(0.5D+d)^3-(0.5D)^3]/(D+2d)^3$.
Using: ε=0.4, d/D=0.08, d=0.000008 m (8 μm) and D=0.0001 m (100 μm), it follows that: $c_{fines}\cong 0.1$.
Thus, a minimum of about p_{clay}=0.1 (10% by volume) of fine particles (< 8 μm) is required for complete coating of the sand particles (63 to 200 μm) by a skin layer of fine particles.
Assuming p_{clay}= 0.1 and a silt-clay ratio of p_{silt}/p_{clay}=2 for natural mixed sediment beds, the critical clay-silt content (< 63 μm) will be about $p_{silt,cr}+p_{clay,cr}=p_{mud,cr} \cong 0.3$. A fully space-filling network will be present for clay-silt contents > 30%. The distance between the sand particles will increase for increasing clay-silt content, see **Figure 2.1**.
If the mud content is below the critical value ($p_{mud}<p_{mud,cr}$), the bed only has weak cohesive or non-cohesive properties. The erosion of the sand particles is the dominant erosion mechanism and the clay-silt particles will be washed out together with the sand particles.
The critical bed-shear stresses for erosion of the clay-silt fraction and the sand fraction can only be determined from laboratory and field tests. The sediment size composition, the percentage (by weight) of clay, silt and fine sand and the bulk densities of the top layer (3 to 5 mm) should be known (measured).

A fully cohesive bed is different from a non-cohesive bed in the sense that the density of the bed is not constant in time due to hindered settling and consolidation processes taking place in the near-bed region. Particle-particle interaction of very fine cohesive particles results in aggregation (flocs) of the particles. In the final stage of the (hindered) settling process near the bed, these flocs become space-filling and form a network structure (gelling structure), which is the onset of the consolidation process (Winterwerp, 1999, 2001). The concentration at the transition from hindered settling to consolidation (or from mobile fluid mud to immobile consolidating mud) is defined as the gelling concentration c_{gel}.
Based on Van Rijn (2007), it is proposed that the gelling concentration can be described by:

$$c_{gel}=(d_{50}/d_{sand})^{\alpha}c_{gel,sand} \qquad \text{with } c_{min}= 0.05 \text{ (volume)} \qquad (2.1)$$

with:
d_{50} = median particle of bed (range of 4 to 63 μm),
d_{sand} = 63 μm=smallest particle size of non-cohesive bed (sand);
$c_{gel,sand}$= $(1-\varepsilon)$=0.65=dry bulk density of sand bed by volume (or =$(1-\varepsilon)\rho_s$=1722 kg/m^3 as dry bulk density by mass), ρ_s = sediment density,
ε = porosity of sand bed ($\cong$0.35 for pure sand bed),
α = empirical coefficient (assumed to be α=1 herein).

Equation (2.1) yields c_{gel}= 0.1 (or 270 kg/m^3) for a mud bed of 10 μm and c_{gel}= 0.05 (or 130 kg/m^3) for a mud bed of 4 μm, the latter value (c_{gel}=0.05) is herein used as the minimum value.
These values are in reasonably good agreement with observations at the mouth of the Amazon in Brazil (Vinzon and Mehta, 2003). They have made detailed concentration and velocity measurements through the mobile fluid mud layer. The gelling/maximum concentrations at the bottom of the mobile hyperpycnal layer were of the order of 200 to 250 kg/m^3. Just above the immobile bed the sediment concentrations were of the order of 200 kg/m^3 decreasing to about 10 kg/m^3 and transported at velocities of 0.1 to 0.7 m/s.
Li et al. (2004) report a value of about 280 kg/m^3 (wet bulk density of about 1200 kg/m^3) as the transition from the mobile fluid mud to the immobile consolidating bed (about 10 μm) for the mouth of the Yangtze Estuary in China.
Consolidation tests of koalinite (< 4 μm) in saline water (Van Rijn, 1993) show that the consolidation process commences at a concentration of about c_{gel}= 150 to 250 kg/m^3. Dankers (2006) found much lower values of c_{gel}= 70 to 90 kg/m^3 for kaolinite (< 4 μm) in saline water.

Erosion
Various types of erosion of muddy beds can be distinguished (see Winterwerp et al., 2012), as follows:

- floc erosion, which is the pick-up of individual particles and small-scale flocs of the fluffy toplayer (millimeters) of the bed by the turbulent vortices of the fluid flow just above the bed, and which occurs for $0.5\tau_{cr}<\tau_b<1.5\tau_{cr}$ with τ_{cr} = erosion threshold stress and τ_b = applied time-averaged bed-shear stress; some erosion may already occur for $\tau_b<\tau_{cr}$ due to higher turbulent stresses;
- surface erosion for $1.5\tau_{cr}<\tau_b<3\tau_{cr}$, which is the simultaneous mobilization of several layers of particles and flocs (failure of the bonds of particles-floc skeleton/network); surface erosion is a drained process as porewater can freely flow away; some swelling of the toplayers is involved; the erosion rate is restricted by the rate of water inflow into the bed;
- mass erosion for $\tau_b>3\tau_{cr}$, which is the erosion of lumps of bed material when the applied fluid stresses are larger than the undrained (remoulded) soil strength of the bed; mass erosion is an undrained process as pore water cannot easily flow inward the bed (pore water underpressures); mass erosion is most often observed for more compacted beds (low permeability).

2.2 Experimental results of critical bed-shear stresses; mud beds

2.2.1 Soft to firm beds

Many studies on the erodibility of pure mud beds in estuarine and marine conditions with particle sizes smaller than 63 μm have been done, see **Table 2.2.1**.

Table 2.2.1 summarizes the critical shear stresses for surface and mass erosion of various types of mud beds with sand percentages <10%. The results of the in-situ field tests are more representative than the results of the laboratory flume tests which involve the handling/preparation of a mud bed.

The critical bed-shear for surface erosion of a weakly consolidated mud bed with a dry bulk density <400 kg/m^3 is of the order of 0.2±0.15 N/m^2. The critical bed-shear for mass erosion of a weakly consolidated mud bed is a factor of 2 to 3 larger.

The critical bed-shear for erosion of a firmly consolidated mud bed with a dry bulk density >800 kg/m^3 is of the order of 1±0.5 N/m^2.

Mud beds	Test method	Dry bulk density (kg/m^3)	Critical bed-shear stress for surface erosion (N/m^2)	Critical bed-shear stress for mass erosion (N/m^2)
Kaolinite (distilled water); Van Rijn 1993	Lab. flume	100-200	0.05-0.2	
Kaolinite (saline water); Van Rijn 1993	Lab. flume	100-200	0.05-0.4	
Dutch lake muds (fresh water); Van Rijn 1993	Lab. flume	100-300	0.1-0.4	0.6-0.7
Gironde subtidal mud; Van 2012	Lab. flume	300	0.2-0.3	0.7
River mud (submerged); Mostafa 2008	Lab. flume	>1000	0.05-0.3	0.3-1.5
China muds; Dou (2000)	Lab. flume	200-400	0.05-0.2	
UK muds; Thorn 1981	Lab. flume	<400	0.05-0.2	
Hong-Kong mud; Mitchener-Torfs 1996	Lab. flume	<400	0.1-0.15	
UK tidal flat muds; Mitchener-Torfs 1996	in-situ ISIS	400	0.05-0.25	
Hudson Bay subtidal mud; Amos 1996	in-situ SC	>1000	0.7-2	
Lunenburg subtidal mud; Sutherland 1998	in-situ SC	100-200	0.05-0.15	
Kongsmark tidal flat mud; Andersen 2001	in-situ EROMES	200-400	0.2-0.4	
Kjelst tidal flat mud; Andersen 2001	in-situ EROMES	200-400	0.2-0.4	

ISIS= Erosion bell, SC= Sea Carousel; EROMES= propeller cylinder

Table 2.2.1 *Critical bed-shear stress for erosion; pure mud beds (d_{50}< 32 μm)*

2.2.2 Stiff clay beds

Erosion resistant clay-type soils can be used to as outer protection of alluvial channel beds, banks and dikes. The clay fraction of the soil has cohesive properties, while it also can retain water. Cohesion is caused by binding forces between the very fine soil particles. The ability of clay to retain water is related to the relatively strong bonding forces between the water molecules and the surface of the soil particles, and because of the very fine pores in the clay resulting in very low permeability values. Also important is the soil structure which is related to the presence of cracks, plant rests and biological activity (**Figure 2.2.1**). Cracking occurs due to shrinking and swelling as a result of the clay becoming wet and dry. Biological activity consists of burrowing animals (worms, insects, moles) and root penetration from vegetation. The soil structure can be expressed by presence of larger and smaller lumps of soil (soil aggregates), which may be held together by plant roots. Clay consists of small particles of solids, water within which compounds are dissolved and gases. The fine particles consist of various clay and quartz minerals. Clay also contains organic materials in the form of the remains of plant and animal organisms (microscopic and larger organisms), fibres, active bacteria and fungi, and organic molecules.

The water pressure in clay above the water table is mainly negative in relation to atmospheric pressure (suction pressure). Clay can suck up water due to this negative pressure. The water pressure only becomes positive above the water table due to precipitation or infiltration of outside water. The suction pressure is determined by a dynamic equilibrium between the gravitational head of water, the height of the water table, and the shape and size of the pores.

Figure 2.2.1 *Soil structure*

The Atterberg limits (flow and plastic limits) are a measure of the plastic properties of soil. A decreasing water content increases the stiffness of the saturated clay. At low water content the clay can behave more like a plastic solid than a thick fluid. The water content at the transition point between thick fluid and plastic clay depends mainly on the binding of water to the clay particles and is known as the flow limit. As the clay becomes drier, the limit is reached at which the cohesive soil can suddenly transform into a plastic state. The water content from this test is termed as the plastic limit. This classification test also gives insight into the binding between particles which involves water. The difference between the flow and plastic limits is known as the plasticity index (PI). For sandy clay, the flow limit is relatively low, and the plasticity index is then usually also low.

Erosion resistant clay-type materials have (Rijkswaterstaat 1996):

- Liquid limit (flow limit) > 45;
- Plasticity Index > 30-40
- Organic content < 5%
- Sand+Gravel content < 40%

The sticky clay types, with a flow limit higher than 45%, are very erosion resistant in running water. Water can run at a speed of 8 m/s along such clay material for several hours with only very minor erosion, provided that the soil is well compacted or has been in the unsaturated zone for a long time.

Many past studies were focused on the critical bed-shear stress of artificially compacted mud beds of pure clay, mixtures of clay, silt and fine sand or pure silt in laboratory flumes (Smerdon and Beasley,1959, 1961; Laflen and Beasley, 1960; Kamphuis and Hall, 1983; Panagiotopoulos,1996; Roberts et al.,1998; Kothyari and Jain, 2008; Le Hir et al., 2008; Jacobs (2011) and Jacobs et al., 2011; Smith et al., 2015 and Wu et al., 2017). In some tests, the mud bed was quite large, while in other tests only small mud cores were pushed upwards through the flume floor at a rate equal to the pickup rate of the recirculating flow (Le Hir et al., 2008; Jacobs, 2011; Jacobs et al., 2011; Smith et al., 2015; Wu et al., 2017). Various methods were used to compact the mud bed mixtures (moulding, drying, rolling, pressing, etc). Dry density values were in the range of 900 to 1900 kg/m^3 for varying percentages of clay, silt and fine sand. The measured critical bed-shear stress of the tested mud beds was often quite high with values up to 20 Pa (Kamphuis and Hall, 1983). Most critical bed-

shear stress values were found to be in the range of 1 to 10 Pa for firmly compacted mixtures with clay percentages of 10% to 50%. Generally, the critical stress was found to increase for increasing bulk density (packing of the bed) and percentage of clay. Often, the pure high-density clay beds had the largest critical stress.

Very early work on firmly consolidated mud beds of clay (mean diameter about 2 μm; 61% clay) and clay-silt (about 20 μm; 14% to 22% clay) was done by **Smeardon and Beasley (1959)** and **Laflen and Beasley (1960)** in a flume.

Smeardon and Beasley (1959) tested natural clay-silt samples in a flume. Eleven soils from the State of Missouri (USA) were selected for testing. These soils were chosen to give considerable range in physical properties, particularly concerning cohesion of the soil and the ease with which the aggregates were dispersed in water. The soil was placed in the flume in a layer of 2.5 inches thick. The remaining portions of the flume bottom were covered with a concrete fill (2.5 inches thick). Approximately 1200 pounds of soil were used for each flume test. The soil was placed in the flume and thoroughly mixed. Lumps of soil were broken up by hand and all foreign particles were removed. The soil was then carefully leveled using a specially constructed template which used the sides of the hy-draulic flume as guides. This assured that the depth of the soil sample was the same as the depth of the concrete fill upstream and downstream from the test section. No attempt was made to compact the soil any more than that which naturally occurred in the process of leveling the bed. The soil was then wetted by slowly admitting water into the flume until the bed was completely soaked. A small amount of coarse gravel was placed on the bed nearest the upper con-crete fill co increase the stability at this critical point. After the bed was wetted, the flume was permitted to drain and the soil sample permitted co dry and consolidate for approximately 20 hours.
The rate of flow was then increased to give a depth of flow over the bed of about 0.05 feet. The process of increasing the flow by increments and recording data was continued until general movement of the bed material was observed. Bed failure was defined at the point at which the bed material was in general movement. The particles were carried down the flume past the transparent flume sides as bed-load. The bed was not considered to have failed until the tractive force was sufficient to cause general movement of the bed material. The highest and lowest value of each soil type are given in **Table 2.2.2**.

Laflen and Beasley (1960) tested natural clay-silt samples from the State of Missouri (USA) in a flume. The soil samples were moulded and satured with water. The beds were artificially compacted to obtain the desired voids ratios in the range of 1 to 2 (dry density in the range of 900 to 1300 kg/m^3). The flow rate was increased by small increments to remove loose aggregates. The flow rate was raised to a value with ongoing erosion of aggregates during some time and used to determine the critical stress for erosion. The critical bed-shear stress (range of 0.6 to 2.5 N/m^2) increased for increasing bulk density. The pure clay bed had the largest critical stress (1.5 to 2.5 N/m^2). The values are given in **Table 2.2.2**.

Kamphuis and Hall (1983) studied the critical bed-shear stress of highly consolidated cohesive mixtures (dry density > 1500 kg/m^3) in a flume with velocities up to 3.5 m/s. Consolidated caly was taken from the bottom of the Mackenzie River in Canada and at some nearby landbased locations. The in-situ water content was in the range of 30% to 50% (dry density in the range of 950 to 1350 kg/m^3. The cohesive samples were artificially compacted in a specially designed press. The dry density of the samples after compaction is herein assumed to the in the range of 1200 to 1600 kg/m^3. Two markedly different highly consolidated soil samples were tested: Series A and B consisting of natural clay-silt samples with p_{clay}=50%-60%, p_{silt}=35%-45% and p_{sand}< 5% and Series D with p_{clay}=15%-35%, p_{silt}=35% and p_{sand}=30%-50%. Test series C, D and E were made from the samples of Series A by mixing with fine sand (d_{50}=0.105 mm). The clay from sample A was dried, pulvarized and mixed with sand and water was added and compacted in a press.

The measured velocity at 3 mm above the bed surface was taken as the critical velocity when erosion was defined to occur as the onset of pit and streak marks (surface erosion) became apparent and used to determine the critical stress.
The onset of surface erosion was observed to occur as:

- generation of pits, parallel streaks;
- removal of flakes;
- general erosion over entire surface.

When erosion was noticed, the velocity was kept contant for 24 to 36 hours. The critical bed-shear stress for erosion was found to be in the range of 10 to 20 N/m^2 for Series A and 1 to 10 N/m^2 for series D with larger sand content. This shows that the critical stress decreases for decreasing percentage of clay.
Some characteristic data of Kamphuis and Hall (1983) are given in **Table 2.2.2**.

Lim (2006) studied the critical shear stress of various stiff clay samples from sites in Australia and USA in a rotating cylinder. In this test, the soil sample is placed between steel plates in a cylinder filled with water, and the shear stress is applied to the soil surface through rotating the cylinder relative to the soil. The torque required to keep the soil sample stationary against the spinning water and cylinder is measured and converted to the shear stress. The data of critical stress are given in **Table 2.2.2**.

Mostafa et al. (2008) studied the erosive behavior of various clay-type soils. Erodibility tests were performed on field samples of natural cohesive soils obtained from several different locations in South Carolina (USA). The cohesive soils were collected from different bridge sites in the form of large undisturbed chunks. The soil chunks were scooped from the bottom and removed as a single piece, wrapped in plastic sheets and placed in a covered container for transportation to the laboratory. In the laboratory, the chunks were cut slowly and carefully with a thin sharp-edged knife to form an even-sized sample that would fit into a sediment indentation in the flume. Surface erodibility tests were performed in a laboratory flume that is 14.5 m long, 1.2 m deep and 0.75 m wide, has constant bottom slope of 0.0033 and an average Manning roughness coefficient of 0.018. The soil sample was placed in a small sediment lift. The sediment surface was flush with the flume bottom. The thickness of the sample was usually between 4 cm and 8 cm. The flow rate was increased in steps and each flow rate was maintained for two hours. If erosion was not observed, the flow was increased and maintained for two hours again. Erosion was observed by means of 1 cm siphon tubes close the flume bottom downstream of the sample. The eroded particles collected in an observation bucket located outside of the flume. Shear stress was calculated from the near-bed Reynolds stresses obtained from the instantaneous velocity measurements using a acoustic doppler velocity probe (ADV).
Particle erosion and mass erosion were observed, see **Figure 2.2.2**. Particle erosion started to occur when fine dispersed clay particles were collected by a siphon in the observation bucket. The erosion mode changes to mass erosion if the bottom shear stress increases sufficiently. Mass erosion was considered to occur in the experiment when small masses (2 to 5 millimeters) of clay were eroded from the soil surface and were collected by the siphon in the observation bucket. Results are given in **Table 2.2.2**.

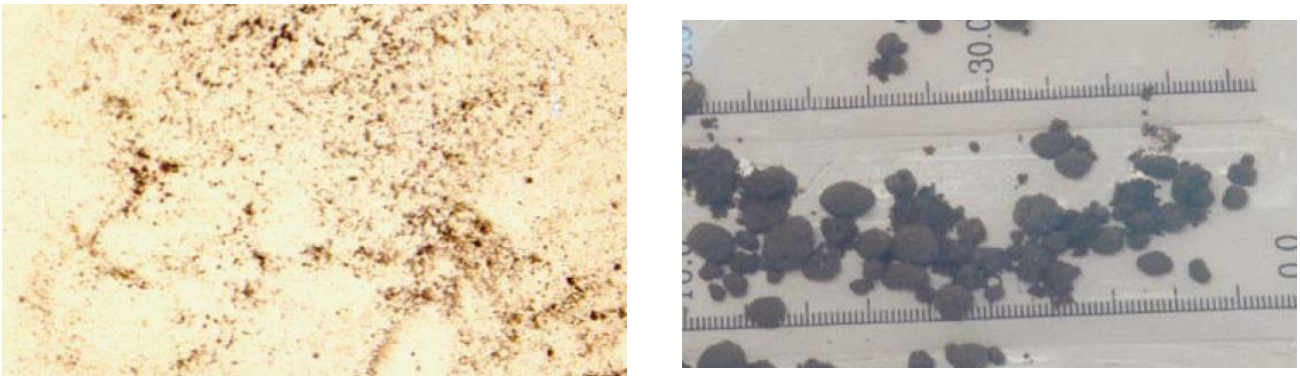

Figure 2.2.2 *Soil fragments related to particle/surface (left) and mass erosion (right)*

Mostafa and Imran (2008) have tested consolidated ***river*** mud samples in a fume with fresh water. The cohesive soil samples were collected from different bridge sites in the form of large undisturbed chunks. During the collection process, the top few centimeters of the soil surface were removed and an area of about 40 cm × 40 cm was marked on the surface. The soil around this perimeter was shoveled to a depth of about 30 cm. The soil chunk was scooped from the bottom and removed as a single piece, wrapped in plastic sheets and placed in a covered container for transportation to the laboratory. The chunk was cut slowly and carefully with a thin sharp-edged knife to form an even-sized sample that would fit into a container in the flume bottom. Surface erodibility tests were performed in a laboratory flume that is 14.5 m long, 1.2 m deep and 0.75 m wide, has constant bottom slope of 0.0033, an average working depth of 0.85 m.
Particle erosion and mass erosion were observed for both field samples and remolded samples. Particle erosion started to occur when fine dispersed clay particles were observed. Particles loosen from the soil surface due to the pressure fluctuations near the bottom that force the water in and out of the soil pores resulting in weakened cohesive bonding between the clay particles. When cohesion forces are overcome, soil particles are pulled out of the surface into suspension and the surface becomes rougher as the particle erosion continues. The effect of lift and drag on the soil surface as well as pressure fluctuations and bottom shear due to turbulence bursts continue to vibrate the protruding particles and more particles leave the soil surface. The erosion mode changes to surface and mass erosion if the bottom shear stress increases sufficiently. Mass erosion was considered to occur in the experiment when small masses of clay were eroded from the soil surface. **Table 2.2.3** shows some results.

Jacobs (2011) studied the erosion threshold stress of various mud-sand mixtures in a small-scale straight test flume (Erodimetre; length=1.2m, width=0.08 m, height=0.02 m). Sediment mixtures were artificially prepared using a dedicated experimental laboratory set-up at a constant temperature of 19°C.
Relatively dense samples were obtained with wet bulk density values > 1800 kg/m^3 (dry density > 1250 kg/m^3). The relatively dense packing prevents segregation of the fractions during the saturation process.
The flume has a sediment container at the bottom where sediment cores can be placed and pushed upwards. Sub samples with a thickness of 2 to 3 cm were used. The surface of the soil sample was horizontally and vertically levelled with the bottom of the flume using four screws. The whole exposed surface area was presumed to contribute to erosion. The bottom of the flume was covered with sandpaper (with a roughness comparable to the applied sand fraction) to decrease differences in roughness with the sample. In practice, nearly no scour was observed at the upstream side of the samples.
A unidirectional flow generated by a re-circulating pump was accelerated step by step (average duration of a step approximately 150 - 200 seconds), until the sample was eroded by a few mm. The flow rate was controlled through a velocity meter in the pump.

Cracks occurred for all soil samples with a dominant clay-water matrix and was characterized by cracks in the surface layer of the soil samples, and by uneven erosion patterns. Before and during the formation of the cracks, individual flocs and sand grains (particle erosion) were simultaneously eroded.
Some test results are given in **Table 2.2.2**, showing an increase of the erosion threshold stress with increasing percentage of mud.

Le Hir et al. (2008) has studied the erosion threshold stress in a small-scale flume of natural mud. He used firmly consolidated sample cores from the intertidal zone of the Mont St-Michel Bay (France).
The top layer of the container was eroded over a few millimeters in 1 to 2 hours. The results clearly indicate the presence of two erosion types: particle/floc erosion and surface erosion.
The dominant size of the sand is about 140 μm. The dominant clay minerals are kaolinite and illite; carbonates are also present. Organic content is low (<2%). Results are given in **Table 2.2.2**.

Wolter et al. (2008) studied the behavior of boulder clay for the outer protection of dykes. A large-scale model test (scale 1 to 1) of the erosion resistance of boulder clay in dikes under wave attack was carried out in the Delta Flume of Deltares (**Figure 2.2.3**). Boulder clay is a clay-like material which has been used in dikes since 1920.
Boulder clay can be found at the edges of glaciers. Boulder clay consists of varying fractions of clay, silt and sand with pieces of shingle. The high gradation ensures a high density of approximately 2000 kg/m^3 and a low water permeability. During the construction phase of the Wieringermeer dike for example the unprotected boulder clay dike was able to withstand flow velocities of 3-3.5 m/s without failure (shear stress of about 20±5 N/m^2 for C=70 to 80 m$^{0.5}$/s). The boulder clay blocks of 10 ton were taken from an old dike and tested in the wave flume. The significant wave height was in the range of 1.1 to 1.6 m with peak periods of 5 to 6 s.
The first 10 minutes of testing caused strong erosion. Individual waves were observed to quarry large chunks of boulder clay out of the slope (resulting in a horizontal erosion length of 1.1 m with an erosion depth of 0.3m). Most of the erosion was found just beneath the waterline. After the first 10 minutes the erosion visibly slowed. The starting erosion revealed stones of 5-15 cm diameter which were embedded in the boulder clay and a large quantity of roots was also revealed. These can have a destabilizing effect on the boulder clay and can reduce the erosion strength. The maximum cumulative (horizontal) erosion length found after testing was about 5,4 m and the maximum cumulative erosion depth (measured vertically) was about 1,9 m after 5 hours of testing.
Using a peak velocity of V=2 m/s and C-values of 70 to 80 m$^{0.5}$/s, the peak shear stresses are about: $\tau_{max}=\rho g (V/C)^2 \cong 7 \pm 2$ N/m^2. Based on this the critical shear stress of boulder clay is at least 5 N/m^2.
The study showed that the behavior of boulder clay is significantly different from clay. Clay erosion is usually faster at the erosion begin but with time diminishes below that of boulder clay.

Figure 2.2.3 *Dutch boulder clay (upper: excavation at local dike; lower: tests in Delta flume)*

Long and Menkiti (2007) have determined the geotechnical properties of Dublin boulder clay (DBC), as follows: Wet bulk density=200-2300 kg/m^3; Moisture Content= 10-15%; Plasticity Index= 15-20% Permeability=10^{-9} -10^{-11} m/s; p_{clay}=10-15%; p_{silt}=15-30%; $p_{sand\text{-}gravel}$=50-70%. The percentage of gravel is relatively large with 30% to 45%.

Mobley et al. (2009) studied the erodibility of stiff clay-type material in a pipeline circuit in which a sediment lift was installed (**Figure 2.2.4**). Analysis of sediment composition showed only 15% < 75 μm (sandy clay), see **Table 2.2.2**. A 1 mm thick portion of soil is pushed into a stream of water and the time required for erosion

noted to establish an erosion rate (mm/hour). Core tube samples were provided from borings for a culvert replacement project in Talladega County, USA. Borings were mostly to a depth of around 4.5 meters. The boring logs described the soil encountered as stiff or very stiff clay with occasional chert pebbles. A common erosion pattern was observed for every tested sample. Silty, clayey emission occurred around the sample edges, and erosion began to occur on the upstream surface. Occasionally large erosion holes/spalls (10 mm) would suddenly occur on the sample surface. Some samples were tested in different way. The testing difference was that the soil was trimmed flush with the bottom of the flume rather than projecting 1 mm into the flow. The critical shear stress was found to be in the range of 0.6 to 1 N/m^2, see **Table 2.1.1**. The erosion rate was about 0.3 mm/hour for τ=1.2 N/m^2 and 1.5 mm/hour for τ=3.2 N/m^2.

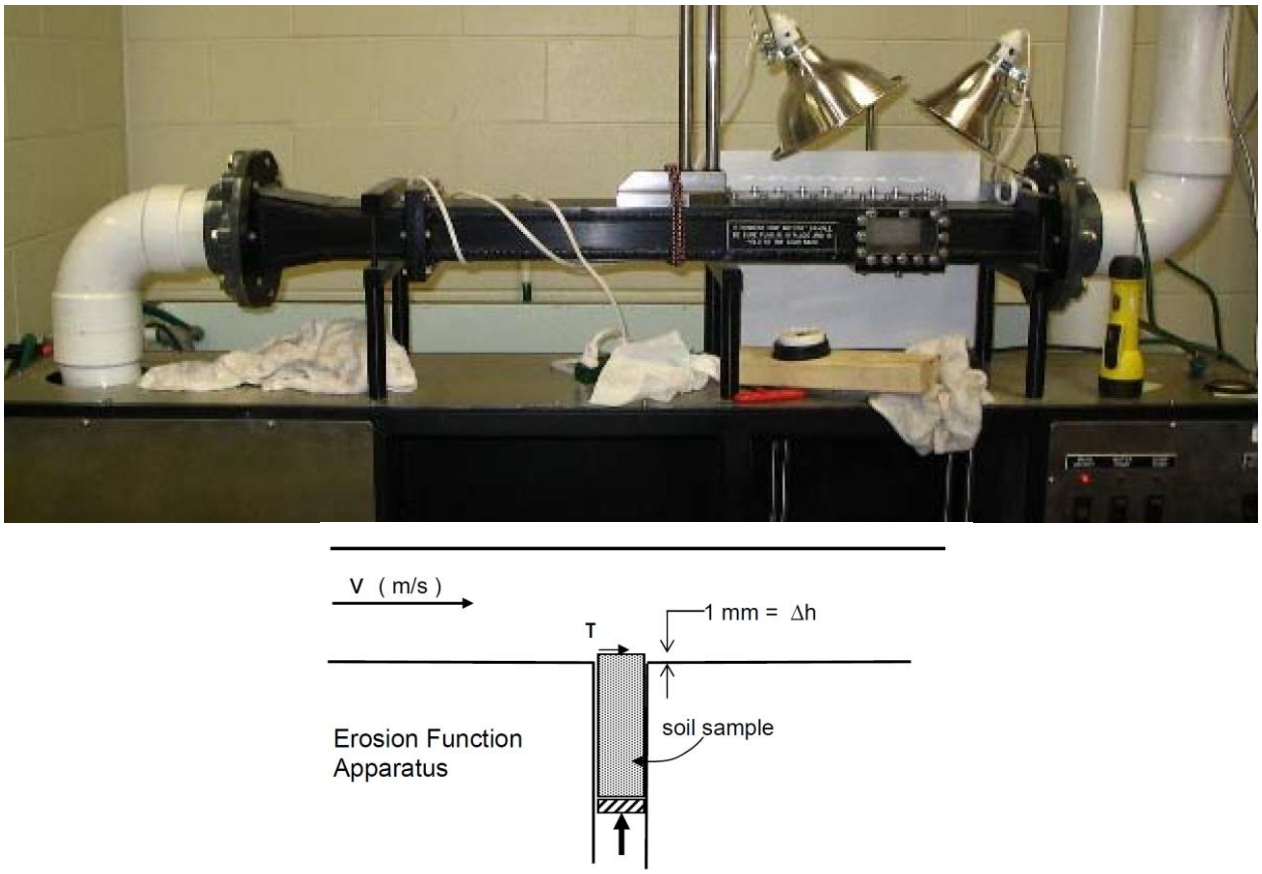

Figure 2.2.4 *Pipeline circuit with sediment lift*

Authors	Sample	Mean size (μm)	p_{clay} (%)	p_{silt} (%)	p_{sand} (%)	Plasticy index (%)	Water content (%)	Dry density (kg/m³)	Critical velocity (m/s)	Critical shear stress (N/m²)
Smeardon and Beasley (1959)		20	15			10		1140		1.0
		20	17			12		1080		1.6
		22	17			7		1010		0.76
		13	24			14		1190		1.05
		10	30			14		1100		2.2
		<10	58			44		955		4.3
		15	23			14		1070		1.6
		15	17			8		1105		1.1
		11	31			18		1140		1.2
		11	25			15		935		1.8
		4	44			30		1010		2.6
Laflen and Beasley (1960)	MS	12	22			4		1140		2.5
	MS	12	22			4		970		1.45
	KS	20	14			4		1120		0.7
	KS	20	14			4		1205		0.5
	KSS	18	24			13		1230		1.1
	KSS	18	24			13		1015		0.5
	MSS	2	61			17		1050		2.3
	MSS	2	61			17		1000		1.6
	MES	20	18			5		1320		2.45
	MES	20	18			5		1030		1.8
Kamphuis and Hall (1983)	A-5		60	35	5	18	37	>1200	1.95	9
	A-9		60	35	5	34	31.5	>1200	2.6	15.7
	A-11		60	35	5	33	33.3	>1200	2.8	18
	B-4		60	35	5	33	31.8	>1200	2.1	11
	C-2		48	35	17	20	30.9	>1200	1.6	6.5
	D-2		36	35	29	11	22.9	>1200	0.95	2.6
	D-3		36	35	29	13	22.6	>1200	1.35	5.0
	E-1		15	35	50	-	20.5	>1200	0.75	1.7
Lim (2006)	Soil A		22	36	42	16	17	1750		2±1
	Soil B		22	9	69	9	12	1945		4±2
	Soil C		35	24	41	18	19	1720		7±2
	Soil D		27	50	23	16	18	1750		>10
	Soil F		16	21	63	8	13	1875		5±2
	Soil G		22	59	21	22	20	1690		5±2
	Soil H		77	9	14	60	41	1250		10±5
	Soil S		27	37	36	19	22	1615		10±5
Mostafa et al. 2008	Soil 1	8.5	40	48	12	22	35	1250		0.55-2.7
	Soil 2	18	26	56	18	15	19	1205		0.3-1.7
	Soil 3	12.2	39	55	6	16	22	1365		0.4-1.6
	Soil 7	6.5	46	46	8	24	33	1460		0.45-2.2
Mobley et al. 2009	Talladega soil		<15%		85	6±1	18±7	1750±150		0.8±0.2
Jacobs 2011		120	2	<8				1200-1600		0.2
		90	7	18				1200-1600		0.5
		70	12	43				1200-1600		0.7
		45	15	65				1200-1600		1
Le Hir et al. 2008			7	13				1200-1600		0.25
			10	20				1200-1600		0.4
			13	27				1200-1600		0.6
			20	40				1200-1600		1.1
			23	47				1200-1600		1.5
			30	60				1200-1600		2.0

Kamphuis and Hall (1983) measured the flow velocity at 3 mm above the bed
Mostafa et al. (2008) have measured critical shear stress for particle and mass erosion; both values are given

Table 2.2.2 *Critical stresses of clay-type soils*

Soil type	Percentage < 2 μm (%)	Percentage < 6 μm (%)	Percentage fine silt (%)	Percentage coarse silt (%)	Wet and dry bulk density (kg/m³)	Critical stress for particle erosion (N/m²)	Critical stress for surface and mass erosion (N/m²)
1	15	40	40	5	1800 (> 1000)	0.05-0.15	0.25-0.5
2	15	25	35	20	1750 (> 1000)	0.05-0.15	0.25-0.5
3	25	40	40	15	1850 (> 1000)	0.05-0.25	0.5-1
7	10	45	40	5	1900 (> 1000)	0.1-0.3	0.8-1.5

Table 2.2.3 *Critical shear stress for particle and mass erosion of consolidated river mud samples; Mostafa and Imran (2008)*

LVRS-Consultancy has studied the erosional behaviour of Boom Clay (2019). Boom clay is a very stiff grey clay with a wet bulk density of about 1900 to 2050 kg/m³ (dry density of 1530 to 1650 kg/m³), plasticity index of about 50%, and a water content between 25% and 30%. The percentage of clay varies in the range of 25% and 60%. The clay minerals consist of about 70% of swelling clay minerals (smectite group: montmorillonite), 15% illite and 10% kaolinite.
The critical bed-shear stress and erosion rates of Boom Clay samples have been determined by means of flume tests. Two modes of erosion have been observed:

- surface erosion of small flakes of 5 to 20 mm at a bed-shear stress of $\tau_{b,cr,se} \cong 1.5$ to 5 N/m²;
- mass erosion of lumps of 10 to 30 mm at a bed-shear stress of $\tau_{b,cr,me} > 5$ N/m².

Three tests with different Boom Clay samples have been done, as follows:

- test BC1: clay lumps of 3 to 5 cm (type M) were cut using a knife from the available dry samples and fitted into the tray compartment of the flume; the flume with clay sample in the tray compartment was filled with water; the test was done the following day after a resting period of about 20 hours; the surface irregularity was similar as that of the supplied samples (**Figure 2.2.5 left** and **2.2.5 right**)
- test BC2: clay lumps were wetted using a very small amount of water and the clay sample was moulded manually and placed in the tray compartment; the clay surface was made flush with the adjacent flume bottom; the test was done the following day after a resting period of about 20 hours; the clay surface has a flaky appearance just before testing with a surface irregularity of about 0.5 mm (**Figure 2.2.5 middle**);
- test BC3: clay lumps (type D) of about 5-10 cm were placed under water in a bucket and were moulded (by slight manual pressing) into a clay slurry; water was poured off and the slurry was placed in the tray compartment and the surface was flattened; the surface roughness was about 1mm (**Figures 2.2.5 lower**).

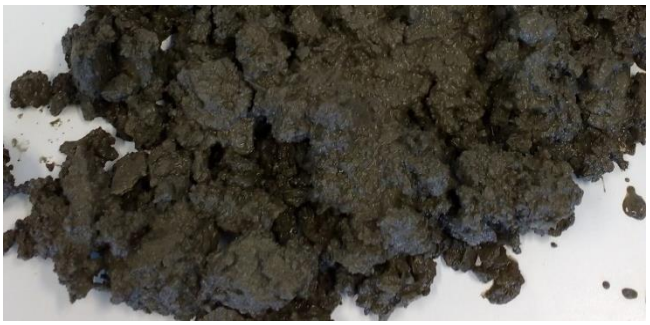

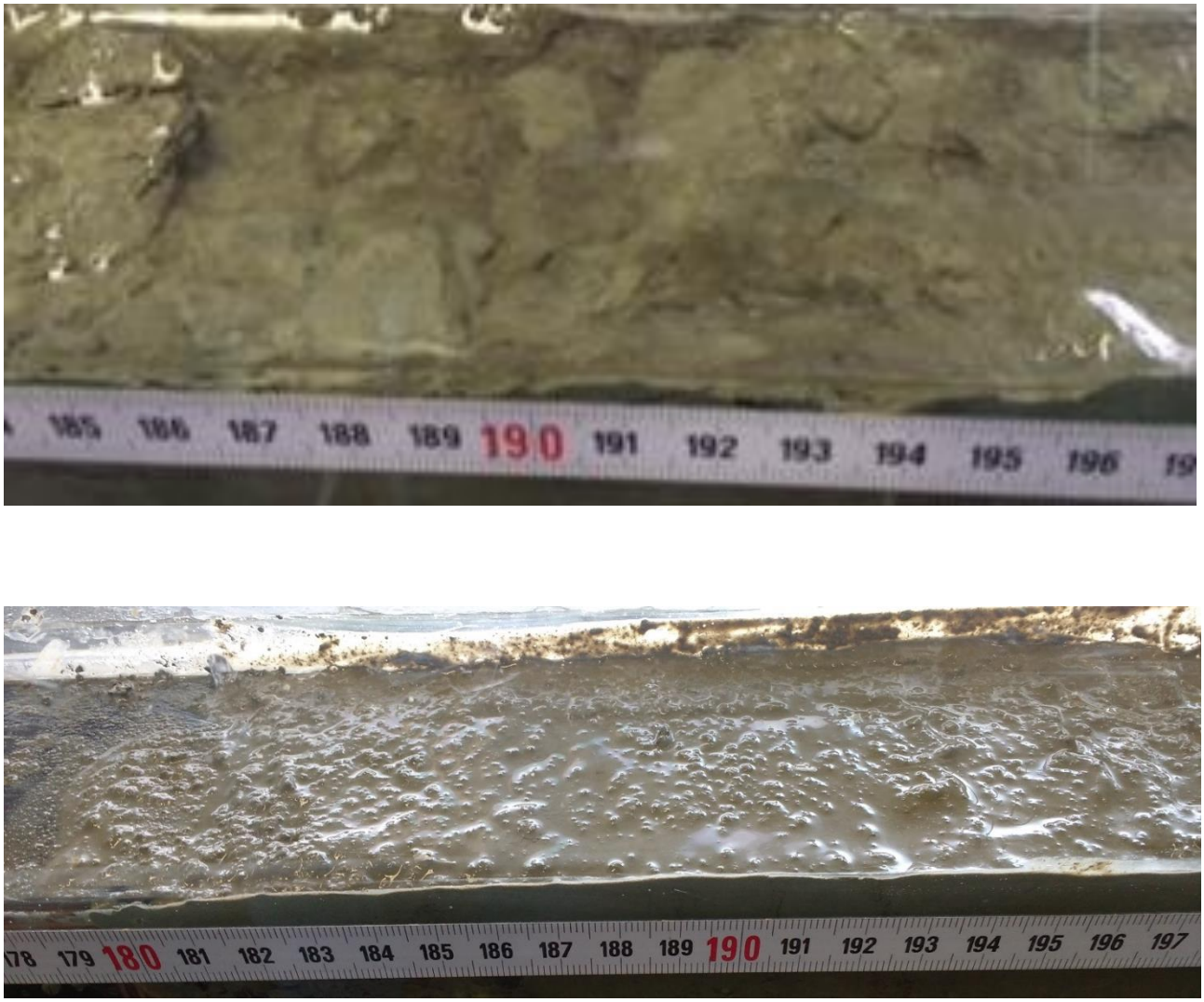

Figure 2.2.5 *Samples of Boom Clay*
Upper Left: dry samples;
Upper Right: : slurry after slight manual moulding of wet samples (soaked in water);
Middle: flaky appearance of Boom clay;
Lower: Slurry of boom clay.

The critical bed-shear stresses of Boom Clay and all available literature data on erosion of clay-type soils from **Table 2.2.2** are shown in **Figure 2.2.6**. The most influential parameters are the percentage of clay (<8 μm) and the dry density of the soil expressing the degree of compaction. The precise type of erosion (particle or surface erosion) is not the same for all literature data. Most data are based on visual observations of particle/surface erosion. Four compaction stages are herein distinguished:

- medium to firm soil with dry density of 400 to 800 kg/m^3;
- firm soil with dry density of 800 to 1200 kg/m^3;
- stiff soil and with dry density of 1200 to 1600 kg/m^3;
- very stiff soil with dry density of 1600 to 2000 kg/m^3.

The critical bed-shear for particle/surface erosion of a firmly consolidated mud bed with a percentage of clay of 15% and a dry density of 800 kg/m^3 is of the order of 1±0.5 N/m^2 (Van Rijn 2020).

The critical bed-shear for erosion of firm soils with a clay percentage <15% is below 1 N/m^2.
The critical bed-shear stresses of very stiff Boom Clay with a percentage of clay of about 55% are in reasonable agreement with the data of the literature for stiff clays. Mostafa et al. (2008) have found critical stresses for surface and mass erosion of 0.5 to 2 N/m^2 for stiff clay from South Carolina (USA) with a clay percentage of 40% to 50% and a dry density of 1350 to 1450 kg/m^3. Boom has a slightly larger dry density than the South Carolina clay of Mostafa et al. (2008) and is also slightly more erosion resistant with critical stresses for surface and mass erosion of 1.5 to 5 N/m^2.

Analysis of the data of **Figure 2.2.6** shows that the critical stress increases for increasing values of the percentage of clay and the dry density. The data can be crudely represented by:

$$\tau_{cr}=\tau_{cr,ref}\,(p_{clay}/p_{clay,ref})\,(\rho_{dry}/\rho_{dry,ref}) \qquad (2.2.1)$$

with: $\tau_{cr,ref}$= critical bed-shear stress (= 1 N/m^2) for erosion of reference soil with $p_{clay,ref}$= 15% and $\rho_{dry,ref}$= 800 kg/m^3.
Computed results of Equation (2.2.1) are shown in **Figure 2.2.6** (red dashed lines) for dry density values of 600, 1000, 1400 and 1800 kg/m^3.

Figure 2.2.7 shows the erosion rate of Boom Clay samples as function of the bed-shear stress. The tests BC1 and BC2 are related to stiff clay lumps under water, whereas tests BC3 is related to a slurry of Boom Clay material.

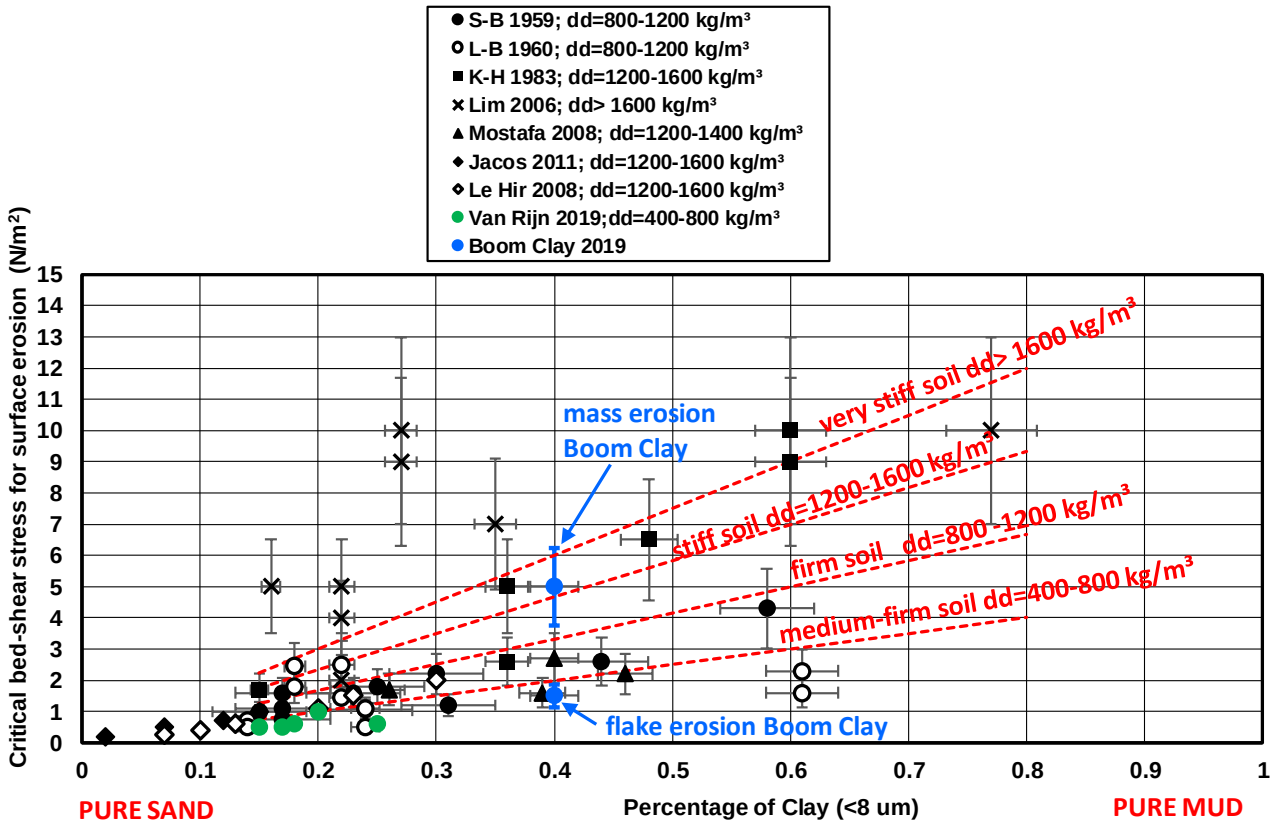

Figure 2.2.6 *Critical bed-shear stress for erosion of firm to very stiff clay-type soils; data literature and Boom Clay*

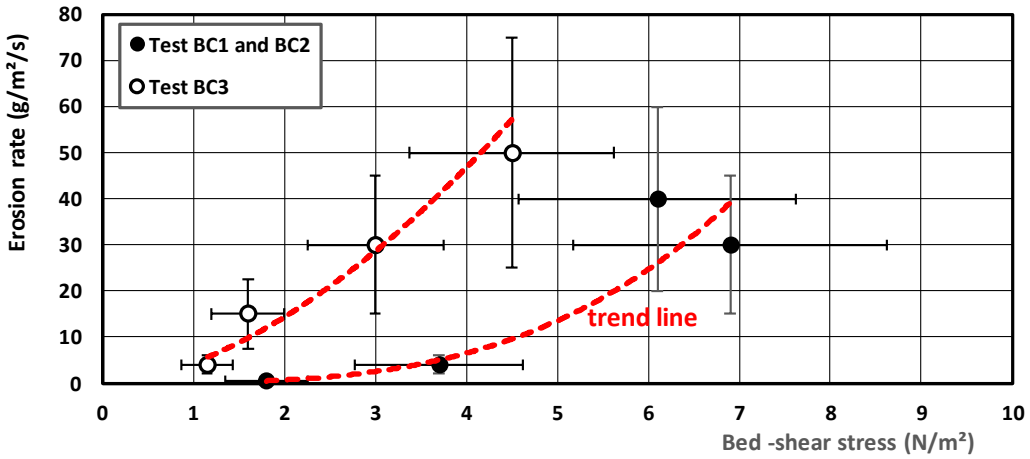

Figure 2.2.7 *Erosion rate of Boom Clay samples*

The critical depth-averaged flow velocity is related to the bed-shear stress by:

$$U_m = C\,[\tau_b/(\rho g)]^{0.5} \qquad (2.2.2)$$

with: U_m=depth-averaged flow velocity, τ_b= bed-shear stress (N/m²); ρ=density of fluid, h= water depth (m), $C = 5.75 g^{0.5} \log(12h/k_s)$ = Chézy-coefficient ($m^{0.5}/s$), k_s= equivalent roughness of Nikuradse (m).
The k_s-value of stiff clay is in the range of 1 mm for a very smooth surface to 10 mm for a surface consisting of soil lumps.
Given a critical bed-stress of surface erosion for Boom Clay of 1.5 N/m², the corresponding depth-mean flow velocities are in the range of 0.8 to 1.2 m/s, see **Figure 2.2.8**. Hence, in the most unfavorable situation, flake erosion of Boom Clay will occur at a depth-mean flow velocity of 0.8 m/s. The erosion rate is estimated to be about 0.5 g/m²/s for these conditions, which is equivalent to about 1 mm/hour.
Based on this, it is concluded that Boom Clay is fairly erosion resistant in flow conditions with velocities smaller than 0.8 m/s.
Flake erosion will occur for velocities of 0.8 to 1.5 m/s.
Mass erosion will occur for flow velocities > 1.5 m/s.

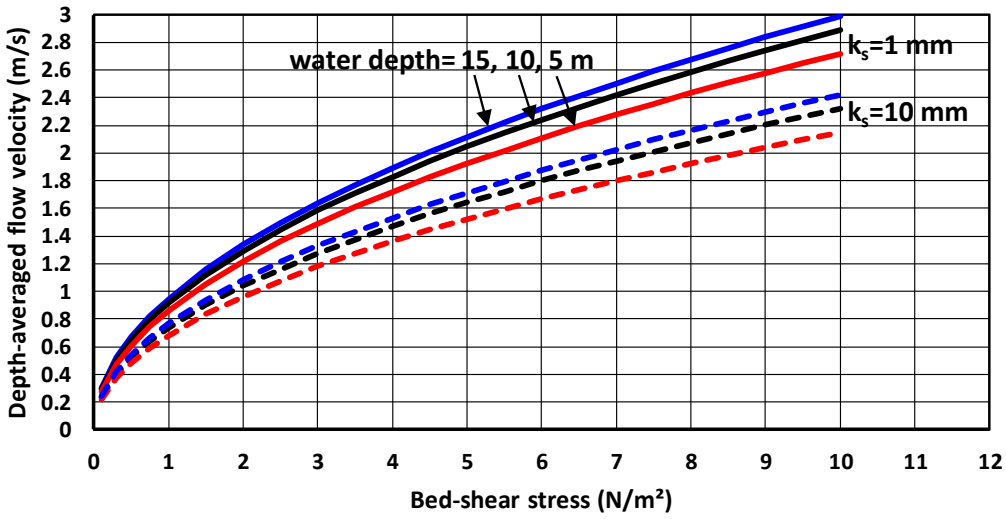

Figure 2.2.8 *Depth-averaged flow velocity as function of bed-shear stress (ρ=1020 kg/m³)*

2.3 Experimental results of critical bed-shear stresses; mud-sand beds

Delft Hydraulics (1989) has determined the critical bed-shear stress (in a flume) of the sand fraction of various natural bed core samples with diameter of about 0.07 m and lengths up to 2.5 m taken (using vibro-core equipment ; May and June, 1989) from the subtidal bed surface near a pipeline site in the Dutch Sector of the North Sea. The samples can be roughly classified as: fine sand (100 to 300 μm), silty sand and clayey silt, silty clay. The percentages of clay and very fine silt (<8 μm) were estimated to be in the range of 0 to 50%. The core samples were splitted in subsamples with a length of about 0.1 m, which were placed in a cylindrical container at the bottom of a laboratory flume. The surface of the sample was exposed to the flow in the flume, which was successively raised until erosion of the bed surface was observed (movement of the sand particles). The critical bed-shear stress for a pure sand sample (200 μm) was found to be about 0.2 to 0.4 N/m^2, which is somewhat larger than the Shields value of 0.2 N/m^2 for sand with d_{50} of 200 μm. This may have been caused by the definition of the critical conditions for initiation of motion as used by the observers: "clear rolling of a considerable number of particles (order of dozens) during the entire test".

Type of sediment sample	Percentage of clay-dominated fraction	Ratio of critical bed-shear stress $\tau_{b,cr,sample}/\tau_{b,cr,pure\ sand}$
Fine sand (non-cohesive)	0%	1
Fine sand with silt (non-cohesive)	0 to 30%	1 to 2
Sand, very silty (cohesive)	30%	2 to 3
Silt, very clayey (grey) (cohesive)	50%	3 to 5
Clay, very silty (brown), (cohesive)	>50%	5 to 10

Table 2.3.1 *Critical bed-shear stress of natural sand-mud mixtures of North Sea (Delft Hydraulics, 1989)*

The critical bed-shear stress was estimated from measured critical velocities assuming a logarithmic velocity profile. The samples with p_{clay}>0.3 (p_{clay}=proportion of clay in bed sample) show a cohesive behaviour with relatively large critical bed-shear stresses ($\tau_{b,cr,sample}/\tau_{b,cr,pure\ sand}$>2). The sandy samples (about 200 μm) show a non-cohesive behaviour with relatively small critical bed-shear stresses ($\tau_{b,cr,sample}/\tau_{b,cr,pure\ sand}$ < 2). The results are presented in **Table 2.3.1**. The results for sand particles (>63 μm) can be roughly represented as: $\tau_{cr,bed}=(1+p_{clay})^3 \tau_{cr,puresand}$.

Mitchener and Torfs (1996) have summarized experimental results on the erodibility of mud-sand mixtures in laboratory and field conditions. Mud (or fines) is defined as clay and silt particles with sizes < 63 μm.
The data, which originate from both laboratory and field experiments, have been used to examine the physical processes behind the erosion behaviour of mud/sand mixtures. It was found that adding sand to mud, or vice versa, increases the erosion resistance and reduces the erosion rates when the critical shear stress for erosion is exceeded. The laboratory beds consist of homogeneously mixed beds and layered beds tested in flume experiments. Natural beds generally have a more layered structure. The field data from various UK-sites concern the in-situ testing of intertidal and subtidal beds using the ISIS-apparatus, which is an in-situ erosion bell consisting of an inverted, curved funnel. Water is drawn from the sides and up through the centre of the funnel by pumping (HR Wallingford, 1992).
Table 2.3.2 shows the critical bed-shear stresses for particle/surface erosion of laboratory and field tests based on the work of Mitchener and Torfs (1996). The field samples may have been affected by biogenic effects (not explicitly measured). The critical bed-shear stress of mud beds is related to the erosion of the topmost layer of 1 mm thick. If the mud percentage is larger than about 30%, a thin mud layer generally may have been present at the bed surface.

The critical shear stress for erosion increases when mud is added to sand, and also when sand is added to mud (mud < 63 μm). The addition of up to 50% sand to a mud bed can typically increase the critical erosion shear stress by a factor of 2. Conversely, the addition of 30% mud to a sand bed can increase the critical shear stress by as much as a factor of 10.

Type of bed	**Percentage sand (150-250 μm)**	**Wet and dry bulk density (kg/m^3)**	**Critical bed-shear stress of particle/surface erosion (N/m^2)**	
			Natural beds of UK sites (intertidal and subtidal)	**Artificial beds (homogeneously mixed)**
Pure mud	0%	1200-1300 (350-450)	0.05-0.25	0.1-0.15 (HK-mud)
Light sandy mud	20%	1300-1400 (450-650)	0.15-0.25	0.15-0.2 (HK-mud)
Sandy mud	40%	1400-1600 (650-950)	0.2-1.0	0.2-0.4 (HK-mud)
Muddy sand	60%	1600-1700	0.4-1.5	0.4-0.8 (K,M,S-muds)
Muddy sand	80%	1700-1800	0.6-1.8	1-3 (K,M,S-muds)
Light muddy sand	90%	1800-1900	?	0.5-1.5 (K,M,S-muds)
Pure sand (150-250 μm)	100%	1900-2000	0.15-0.2	0.15-0.2 (K,M,S-muds)

HK= Hong-Kong, S=Scheldt, K=Kaolinite, M=Montmorillonite

Table 2.3.2 *Critical bed-shear stress of mud-sand mixtures (laboratory-field, Mixener and Torfs 1996)*

The critical shear stress at mud percentages of about 30% depends on the grain size of the sand (which anchors the critical shear stress at the 100% sand point) and the cohesive properties of the mud. The top layer may then consist of a thin muddy layer.
The addition of mud to sand significantly increases the critical erosion shear stress with a maximum value occurring at a mud content of between 30% and 50% by weight. If enough mud is added to sand (>50%), then the sediment mixture behaves as if it were a mud. It should also be realized that the bulk density depends on the compaction time scale for mixtures with mud contents > 30% (weakly and firmly consolidated bed mixtures can be present for mud contents > 30%).

Panagiotopoulos et al. (1997) have determined the critical erosion velocity of sediment mixtures under currents and under waves. The sediment mixtures consisted of fine sand (152 μm and 215 μm) and estuarine mud ranging from 0 to 50%. The pure clay content (< 2 μm) of the mud varies from 0 to 18%. The results are given in **Table 2.3.3.**. The critical erosion velocity of sand shows an increase of 30% to 50% for a mud content of 50%. The wave tests show that the critical wave-related bed-shear stress of sand is not affected for mud contents smaller than about 30%.

Mud content and pure Clay (<2 μm) content	Sand 152 μm			Sand 215 μm		
	Critical velocity at 4 mm above bed (m/s)	Current-related bed-shear stress (N/m^2)	Critical wave-related bed-shear stress (N/m^2)	Critical velocity at 4 mm above bed (m/s)	Current-related bed-shear stress (N/m^2)	Critical wave-related bed-shear stress (N/m^2)
0% (0%)	0.14	0.094	0.05	0.125	0.074	0.045
10% (3%)	0.145	0.098	0.05	0.135	0.085	0.045
20% (7%)	0.155	0.108	0.05	0.14	0.092	0.045
30% (11%)	0.16	0.114	0.05	0.145	0.096	0.045
40% (15%)	0.17	0.132	0.08	0.16	0.114	0.07
50% (18%)	0.18	0.144	0.10	0.18	0.142	0.07

Table 2.3.3 *Critical conditions (laboratory) for erosion of sand-mud mixtures (Panagiotopoulos 1997))*

Roberts et al. (1998) have done experiments on initiation of motion of cohesive beds consisting of very small quartz particles (< 63 μm) with relatively high wet bulk densities (1600 to 1900 kg/m^3).
The sediments that were used in the tests consisted of quartz particles (99.5% pure) with mean diameters, *d* of 5.7, 14.8, 18.3, 48, 75, 125, 222, 432, 1,020, and 1,350 μm. Each sediment had a fairly narrow size distribution. These particle size distributions were measured by means of a Malvern particle sizer after thorough disaggregation of any flocculated sediments in a Waring blender.
In order to obtain different bulk densities for each sediment for the erosion tests, sediment cores were prepared as follows. Thirty to thirty-eight liters of each wet sediment were placed in a 45 liter cylindrical container and mixed with water for 15 to 30 min until the sediment-water mixture was homogeneous.
The amount of water added was enough to allow the mixture to be fluid, but care was taken to also keep the mixture thick so that stratification of the sediment due to differential settling of the particles did not occur. The sediment mixtures were then poured into coring tubes generally to a depth of 20 cm. These cores were then allowed to compact for 8 h to 124 days. Duplicate analysis cores were checked for repeatability and to ensure uniformity in particle size with depth. In order to determine the bulk density of the sediments at a particular depth and compaction time, the sediment analysis cores were frozen, sliced into 3 to 4 cm sections, and then weighed (wet weight). They were then dried in the oven at approximately 75°C for 2 days and weighed again (dry weight).
For each sediment and compaction time, erosion rates were determined by means of flume tests at shear stresses from 0.2 to 6.4 N/m^2. This flume is essentially a straight flume that has a test section with an open bottom through which a rectangular cross section coring tube containing sediment can be inserted. This coring tube has a cross section that is 10 by 15 cm and, in the present experiments, is 20 to 40 cm long. Water is pumped through the flume at varying rates and produces a turbulent shear stress at the sediment-water interface in the test section. This shear stress is known as a function of flow rate from standard pipe flow theory. As the shear produced by the flow causes the sediments in the core to erode, the sediments are continually moved upward by the operator so that the sediment-water interface remains level with the bottom of the test and inlet sections.
As the rate of flow of water over a sediment bed is increased, there is a range of velocities (or shear stresses) at which the movement of the smallest and easiest-to-move particles is first noticeable to an observer. These eroded particles then travel a relatively short distance until they come to rest in a new location. This initial motion tends to occur only at a few isolated spots. As the flow velocity and shear stress increase further, more particles participate in this process of erosion, transport, and deposition, and the movement of the

particles becomes more sustained. Because of this gradual increase in sediment erosion as the shear stress increases, it is difficult to precisely define a critical velocity or critical stress at which sediment erosion is first initiated. More quantitatively and with less ambiguity, a critical shear stress can be defined as the shear stress at which a small, but accurately measurable, rate of erosion occurs. This rate of erosion was chosen to be 10^{-4} cm/s; this represents 1 mm of erosion in approximately 15 min. Since it would be difficult to measure all critical shear stresses at an erosion rate of exactly 10^{-4} cm/s, erosion rates were generally measured above and below 10^{-4} cm/s at shear stresses that differ by a factor of two. The critical shear stress can then be obtained by interpolation between the two. This gives results with a 20% accuracy for the critical
In the experiments, sediments consisting of the larger particles consolidated relatively rapidly (seconds to minutes) and attained a relatively high wet bulk density (1850 to 1950 kg/m^3), which then did not change appreciably over several months. In contrast, sediments consisting of the finer particles consolidated slowly and did not reach a steady-state density over a period of several months; the range of bulk densities attained during this period of time (1650 to 1950 kg/m^3) was greater than for the larger particles.

Natural sediment beds consisting of sand, silt and clay (and organic material) have much lower densities, particularly when organic materials are involved (1100 to 1300 kg/m^3; Li et al., 2004). Based on the results of Roberts et al., it can be concluded that the critical bed-shear stress is minimum for about 63 μm (**Figure 2.3.1**). Cohesive effects become important for particles finer than 63 μm, which is manifest from the increase of the critical bed-shear stress for decreasing particle size. Experimental results of Roberts et al. for particle (quartz) sizes of 6, 15 and 50 μm in a bed with bulk density of about 1650 and 1700 kg/m^3 are shown in **Figure 2.3.1** with critical bed shear stresses increasing from 0.08 N/m^2 to 0.25 N/m^2 for particle sizes decreasing from 50 to 6 μm. Their experiments also show that the critical bed-shear stress is affected by the packing of the bed (bulk density) and by the presence of clay particles. The presence of 2% Bentonite in a sand bed of relatively high wet density (1900 to 2000 kg/m^3) results in an increase of the critical bed-shear stress by a factor of about 1.5. The representative particle size of fine sediment beds smaller than about 32 μm is not well defined because most of the particles will not be eroded as single particles. Roberts et al. (1998) report that the silt particles (<32 μm) are eroded as aggregates (or chunks; mass erosion) which disintegrate as they are transported downstream.

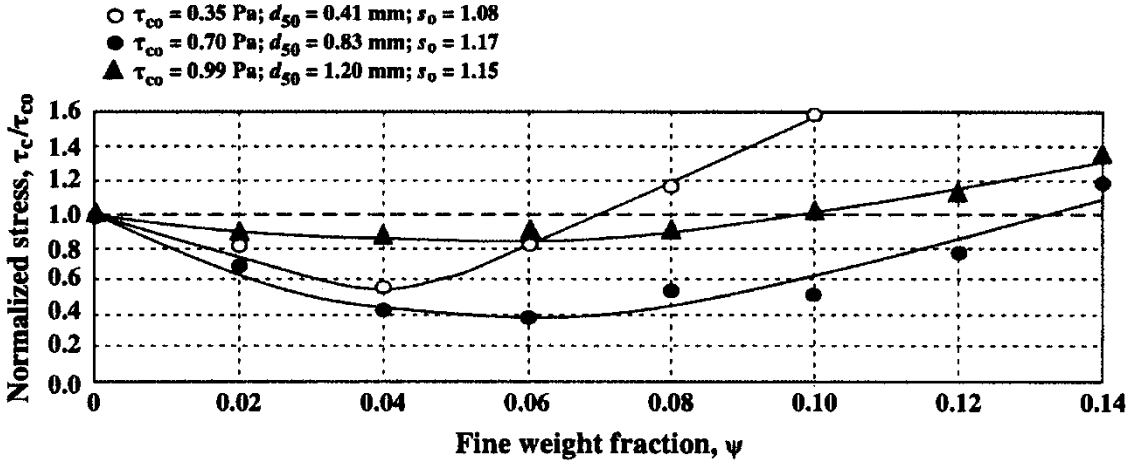

Figure 2.3.1 *Effect of clay fraction on critical bed-shear stress of sand particles(ratio of critical stress and critical stress of pure sand on vertical axis); Barry et al. (2006)*

Barry et al. (2006) have found a lubrication effect of clay particles on sand grain erosion. Minor changes in the mass physical properties of submerged sand beds can have significant consequences relative to bed stability against erosion. To examine the effect of small amounts of clay-sized particles in bed pore water on the critical shear stress for the erosion of sand grains, flume experiments were carried out on the erosion of quartz sand beds impregnated with clay particles. Starting with no clay, as the clay mass fraction (between 0 and 15% of the total mass of the samples) was increased, the critical shear stress of the sand particles at the top of the bed was found to decrease (probably due to lubrication effects) below the value for pure sand ($\tau_{b,cr,o}$) by about 40% to 50% and then reverted to $\tau_{b,cr,o}$ at a concentration $c_{clay,pore}$ and continued to increase (probably due to binding effects) as the mass fraction of clay was increased further. Post-experimental analysis suggests that $c_{clay,pore}$ is approximately equal to the pore space-filling clay fraction above which sand erosion is significantly influenced by clay. A sand bed sample has a porosity of about 0.4 or 400 liters per m^3, which can be filled with a mixture of clay (< 4 μm) of about 240 liters of clay (about 640 kg assuming porosity of 0.4 of the clay mixture) and 160 liters of pore water (40% of 400 liters) yielding an overall porosity of 0.16 of the clay-sand mixture. The wet bulk density of the clay-sand mixture is 1600 kg sand plus 640 kg clay plus 160 kg water or about 2400 kg/m^3. The maximum clay fraction filling the pores of the sand bed only is about 24% by volume (240 liters of clay/1000 liters) or 26% by mass (640/2400). The reduction effect is supposed to be caused by slider-bearing type lubrication due to the viscosity of the clay-laden interstitial fluid. It may also be a factor in the estimation of bed stability when biological activity in the benthic boundary layer introduces fine particles in clean sand beds. The reduction effect may only occur for the sand particles on top of the mixture bed. Sand particles buried in the bed may experience an increase of the critical bed-shear stress for erosion.

Jacobs (2011) has studied the erosion threshold stress of various mud-sand mixtures in a small-scale straight test flume (Erodimetre; length=1.2m, width=0.08 m, height=0.02 m; see **Figure 2.3.2** ; Le Hir et al., 2008.
Sediment mixtures are artificially generated using a dedicated experimental laboratory set-up at a constant temperature of 19°C. First, the individual fractions are oven-dried to disaggregate the material. Next, sand, silt and clay are manually mixed for around 10 minutes. The dry mixture is subsequently placed in a cylindrical container with a removable bottom-lid. Small holes (diameter = 3 mm) in the bottom and top-lid allow the passage of water and gas; paper filters at both ends retain the grains. The containers with dry sediments are placed in an exsiccator to remove air by lowering the pressure to 200 mbar. Next, the exsiccator is filled with CO_2, after which the pressure is lowered again to replace enclosed air in the voids of the mixture with CO_2. Subsequently, mixtures are left for 24 hours in the exsiccator, in which a layer of water is present. The combination of the low pressure (reduced surface tension), 100% humidity and the attractive forces of the negatively charged clay particles enables water molecules to activate the clay particles in the smallest pores. The second part of the saturation process concerns the placement of a layer of 10 cm de-aired and demineralised water on top of the soil samples using the difference between the atmospheric and reduced pressure within the exsiccator. Subsequently, water percolated through the mixture, thereby completing the saturation procedure. The pressure induced by the water column corresponds with the target strength of the soil samples. Therefore, no consolidation is anticipated. The volume of water (about 0.5 litre) is sufficiently large to fill all pores and to dissolve all enclosed gas.
The saturation degree of the soil samples treated this way is about 100%. Using this method, relatively dense samples are obtained with wet bulk density values > 1800 kg/m^3. The relatively dense packing prevents segregation of the fractions during the saturation process. This experimental procedure generates reproducible and isotropic soil samples. This implies the absence of pore water pressure gradients, which would initiate swelling or consolidation. Particle size distributions were determined by using the Sedigraph and Malvern laser-diffraction methods.
The flume has a sediment container at the bottom where sediment cores can be placed and pushed upwards. Sub samples with a thickness of 2 to 3 cm were used. The surface of the soil sample was horizontally and vertically levelled with the bottom of the flume using four screws. The whole exposed surface area was presumed to contribute to erosion. The bottom of the flume was covered with sandpaper (with a roughness

comparable to the applied sand fraction) to decrease differences in roughness with the sample. In practice, nearly no scour was observed at the upstream side of the samples.
A unidirectional flow generated by a re-circulating pump was accelerated step by step (average duration of a step approximately 150 - 200 seconds), until the sample was eroded by a few mm. The flow rate was controlled through a velocity meter in the pump. The volume of eroded sand was monitored at a sand trap downstream of the sediment sample, at the end of each velocity step. After the test, the total dry-mass of this material was determined. The grain size distributions of both the original soil samples and the sand trap material were determined using a laser-granulometer.
Cracks occurred for all soil samples with a dominant clay-water matrix and was characterised by cracks in the surface layer of the soil samples, and by uneven erosion patterns. **Figure 2.3.3** shows that both radial cracks (mostly) and cracks parallel to the flow direction exist (longitudinal cracks). Before and during the formation of the cracks, individual flocs and sand grains (particle erosion) were simultaneously eroded. Also some aggregates of sediment randomly eroded from the cracks, which generated somewhat less accurate sand trap and concentration readings. Most soil samples did not exhibit either of the features during the surface erosion of individual sand and mud particles. Sand arrives in the sand trap within seconds after erosion. Identical behaviour was found for soil samples with kaolinite and bentonite.
Some test results are given in **Table 2.3.4**, showing an increase of the erosion threshold stress with increasing percentage of mud.

Tests	Percentage sand (%)	Percentage silt (%)	Percentage clay (%)	Percentage mud < 63 μm (%)	Mean sediment size (μm)	Wet bulk density (kg/m^3)	Critical bed-shear stress of particle/surface erosion (N/m^2)
1	90-100	< 8	<2	10	100-150	>1800	0.18±20%
13, 14	75	18	7	25	80-100	>1800	0.5±30%
18, 19	45	43	12	55	60-80	>1800	0.7±40%
5	20	65	15	80	30-60	>1800	1±40%

Table 2.3.4 *Critical bed-shear stress of particle/surface erosion of highly-consolidated mud-sand mixtures in laboratory flume (Jacobs 2011)*

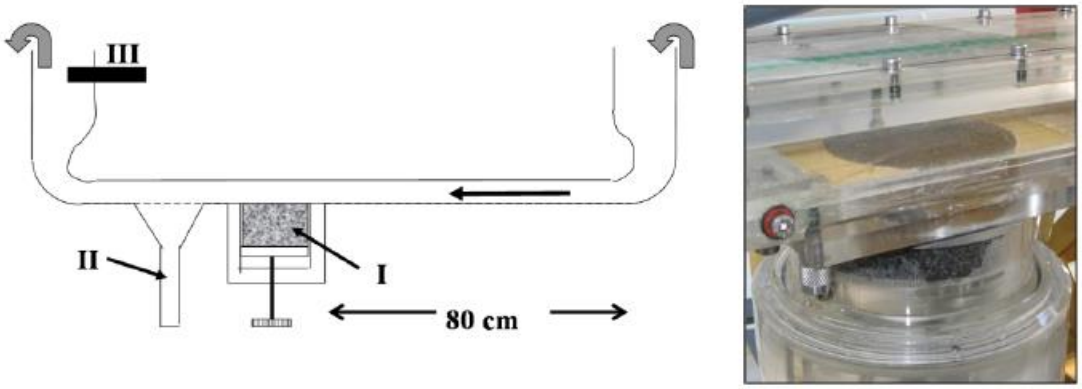

Figure 2.3.2 *Small-scale test flume with sediment lift (I=lift; II=trap)*

Figure 2.3.3 *Examples of eroded surfaces with cracks (Jacobs 2011)*

Le Hir et al. (2008) has studied the erosion threshold stress in a small-scale flume (see **Figure 2.3.2**) of natural mud. He used firmly consolidated sample cores from the intertidal zone of the Mont St-Michel Bay (France). The top layer of the container was eroded over a few millimeters in 1 to 2 hours. The results clearly indicate the presence of two erosion types: particle/floc erosion and surface erosion.
The dominant size of the sand is about 140 μm. The dominant clay minerals are kaolinite and illite; carbonates are also present. Organic content is low (<2%). Results are given in **Table 2.3.5**.

Percentage mud < 63 μm (%)	Critical bed-shear stress of particle/surface erosion (N/m^2)
20	0.25±20%
30	0.4±20%
40	0.6±20%
60	1.1±25%
70	1.5±25%
90	2.0±30%

Table 2.3.5 *Critical bed-shear stress of erosion of consolidated mud-sand mixtures (Le Hir et al. 2008)*

Houwing (2000) has used an in-situ erosion flume to determine the critical bed-shear stress for erosion of sand-mud mixtures at tidal mud-sand flats in the southern Wadden Sea (The Netherlands). His results are presented in **Table 2.3.6**. The critical bed-shear stress for an almost pure sand bed (d_{50}= 80 μm, d_{10}=65 μm, d_{90}=110 μm; p_{clay}=4%) is about 0.18 N/m^2, which agrees rather well with the Shields-value for fine sand of 110 μm. The critical bed-shear stresses for 7 stations with p_{cfs} of about 20% are in the range of 0.1 to 0.18 N/m^2. The critical bed-shear stress for 1 station with p_{clay}=35% is larger than 0.5 N/m^2 (outside maximum range of in-situ erosion flume). For p_{clay}<25% the critical bed-shear stress for erosion is hardly affected by the presence of clay, which is an indication of the non-cohesive behaviour of most samples. One sample with p_{clay}=35% shows a typical cohesive behaviour. Hence, the critical clay-silt content for this site (tidal mud-sand flat) is about $p_{clay,cr}$= 30%. The erodibility of the bed surface decreases with increasing clay-silt content (**Table 2.3.6**).

Type of sediment sample	Percentage of clay + fine silt materials	Critical bed-shear stress of particle erosion (N/m^2)	Erodibility of bed ($kg/m^2/s$)
1 station (18) (non-cohesive)	4%	0.18	0.003
1 station (12) (non-cohesive)	8%	0.15	0.002
7 stations (non-cohesive)	13 to 23%	0.10-0.18	0.00008 to 0.002
1 station (10) (cohesive)	35%	>0.5	0.00006

Table 2.3.6 *Critical bed-shear stress of natural sediment mixtures for intertidal flats (Houwing, 2000)*

Amos et al. (1997) have studied the stability and erodibility of fine-grained sediments on the foreshore and upper foreslope of the tidal Fraser River delta (Canada) using the *in situ* sea carousel flume, see **Figure 2.3.4**. The erosion threshold varied between 0·1 and 0·5 N/m^2 and was proportional to the sediment wet bulk density. Three erosion types were observed:

- Type IA-erosion was a surface phenomenon caused by the presence of a thin organic (fluffy) layer and occurred at current speeds less than 0·3 m/s;
- Type 1B-erosion (asymptotically decaying with time) characterized the mid portions of each erosion-time series, and occurred at current speeds of 0·3–0·9 m/s; video observations showed that Type I-erosion is largely the result of entrainment of small aggregates and flocs;
- Type I/II-erosion (transitional) was largely found on the foreslope, and occurred at current speeds in excess of 0·8 m/s; Type II erosion was the result of enlargement of surface irregularities, and subsequent undercutting and release of large aggregates (mass erosion).

Sediment stability was measured at 12 stations across Sturgeon Bank. Stations were occupied on the inner littoral mud flat, the littoral sand flat and the sub-littoral foreshore muds. Stations 1, 2, 3, 7, 8, 13 and 14 were situated at mud-dominated locations; the other stations were at sand-dominated locations. Stations 7 and 8 were situated on the steeply dipping upper foreslope of the Fraser River delta at a depth of 15 m below lowest low water. The foreshore mud flat is bioturbated and pelletized by a diverse invertebrate infauna. The tides in the region are mixed semi-diurnal reaching 4·8 m in range. Surface currents over the foreslope flow northward at a rate of 0·3–0·5 m/s. The region is relatively sheltered from waves.
Sea Carousel was deployed from a floating pontoon during the marine inundation of the tidal flat, thereby encapsulating the natural, saturated substrata and the overlying epibenthic water mass.

Stations	Percentage sand (%)	Percentage silt (%)	Percentage clay (%)	Percentage organics (%)	Mean sediment size (μm)	Wet and dry bulk density (kg/m^3)	Critical bed-shear stress of particle/surface erosion (N/m^2)
2	5	70	25	3	8	850	0.15
1 and 14	10	70	20	2	22	1040-1270 (50-450)	0.2-0.4
13	20	50	25	3	13	1170 (450)	0.2-0.5
3 and 7	35	45	20	5	20	950-1040 (<50)	0.1-0.25

Table 2.3.7 *Critical bed-shear stress of surface erosion at intertidal mud flats of tidal Fraser River, Canada (Amos et al., 1997)*

Sea-bed samples of the foreshore stations were collected during tidal exposure of the flats. Bulk samples were collected by using a gravity corer and by skimming the surface veneer of sediment with a spatula. Bottles of known volume were used to collect samples for water content and wet bulk density. At some stations the wet bulk density was smaller than 1000 kg/m^3, which is an indication for the presence of bioturbations, organic materials and flocculated aggregates.
The results are shown in **Table 2.3.7**. The sedimentation rate is a dominant factor influencing sediment stability in the region. At locations where the sedimentation rates are relatively high, the bulk density and the threshold stresses are relatively low (0.15 to 0.25 N/m^2).

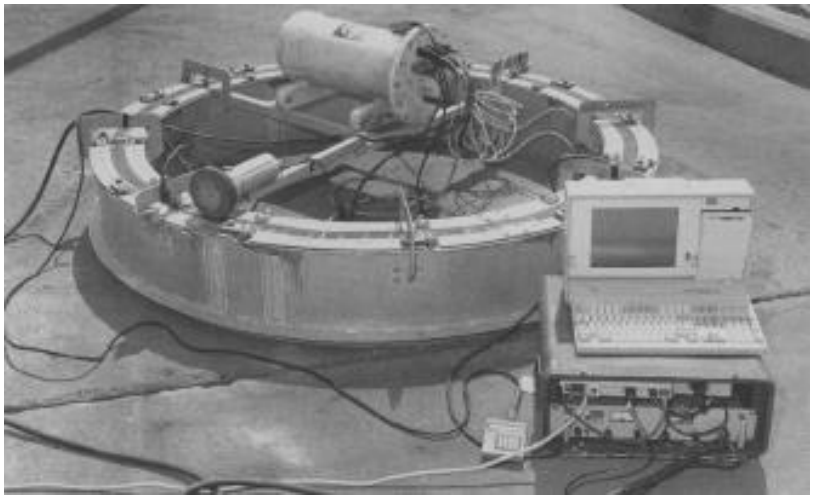

Figure 2.3.4 *In-situ sea carousel flume (diameter=2 m; width=0.15 m, height=0.3 m)*

Tolhurst et al. (2000) have studied the critical shear stress for erosion at various intertidal mudflats using various methods. Measurement results of intertidal mudflat erosion thresholds from in-situ and laboratory erosion instruments were compared for cases with minimum (negligible) chlorophyll content. In an initial experiment, box cores were collected from the Humber estuary mudflats (April 1995) and transported back to the laboratory for measurement in a linear flume. These cores suffered visible disturbance during transport to the laboratory and their erosion thresholds were considerably higher than in-situ data obtained by the sea carousel erosion apparatus. Samples from the Sylt-Romo Bight (June 1998) were collected and transported in a manner that minimised disturbance. The stability of these cores was measured with the EROMES laboratory erosion device based on a rotating propeller in 10 cm diameter perspex cylinder and compared to in-situ measurements taken with the CSM-erosion device based on vertical water jet to erode the sediment surface. ISIS is an in-situ erosion bell consisting of an inverted, curved funnel. Water is drawn from the sides and up through the centre of the funnel by pumping.

When disturbance of cores was minimised, in-situ and laboratory erosion thresholds were comparable. Basic data sets from the Sylt-Romo Bight are given in **Table 2.3.8**. Critical shear stresses are relatively high for Chlorophyll contents > 20 mg/m^2. Biofilms (microphytobenthos) have almost no effect on the critical bed-shear stress for chlorophyll contents < 20 mg/m^2.

Location	**Fraction < 63 μm (%)**	**Wet and dry bulk density (kg/m^3)**	**Chlorophyll a content (mg/m^2≅ μg/g)**	**Critical bed-shear stress of particle erosion at erosion rates < 0.01 g/m^2/s (N/m^2)**
B	15-25	1600-1700 (> 1000)	10-25	0.25-0.40
M	50	1350-1450 (550-750)	20-30	0.45-0.50
Ko1	40	1560 (900)	15	0.2
Ko2	80	1270 (450)	30-40	0.4-1.5

Table 2.3.8 *Critical bed-shear stresses based on EROMES erosion instrument, Sylt-Romo Bight, Germany (Tolhurst et al. 2000)*

Figure 2.3.5 show the critical bed-shear stress for particle erosion as function of bulk density for samples with a low (neglible) Chlorophyll content (< 20 mg/m^2). Pure mud samples have a relatively low dry bulk density (< 400 kg/m^3). The dry bulk density increases with increasing fine sand content. The results of various different instruments are in reasonable agreement.
Tolhurst et al. (2000) concluded that precautions should be taken to minimise disturbance during transport. Transportation times should be kept to a minimum, and measurements should be made within a few hours of collection.

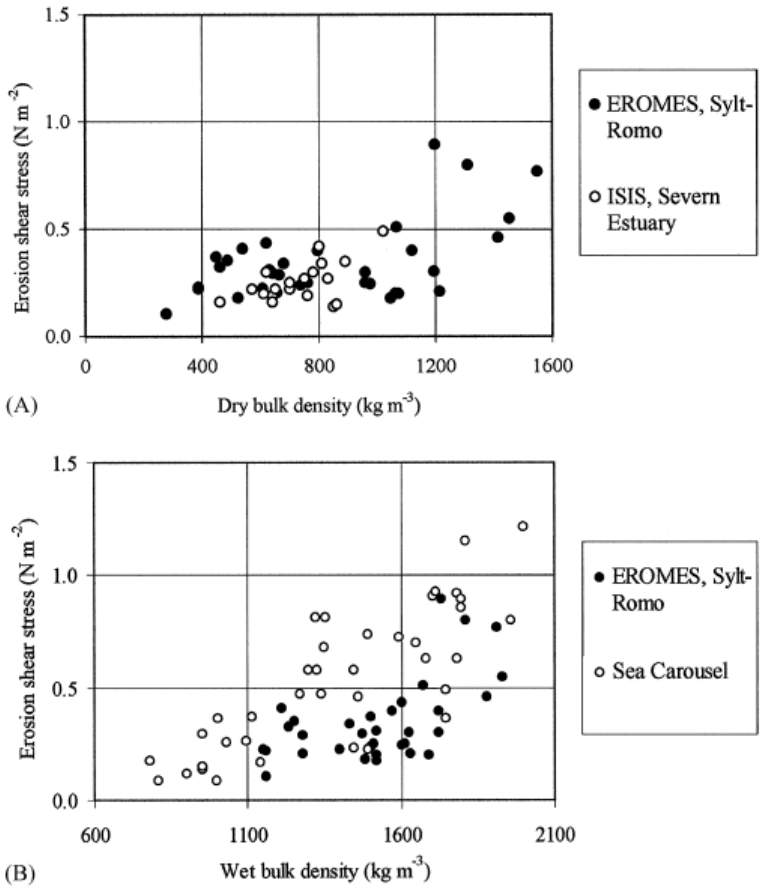

Figure 2.3.5 *Critical bed-shear stress for particle erosion as function of bulk density (samples with chlorophyll < 20 mg/m²)*

German authorities (Bauamt, 1987) have performed a research project in the period 1982 to 1987 to study the tidal flow velocities and mud concentrations in the subtidal channel near the ferry landing Nessmersiel. The Nessmersiel channel has a length of 1200 m outside the landing pier. A long guiding dam with crest level varying between 0.5 and 0.9 m NN is present on the west side of the channel. The channel length between the ferry pier and the gate station (of the inland flushing lake) under the main road is about 500 m. The channel width is about 30 to 40 m. The channel bed consists of muddy/sandy sediments. Various small-scale creeks running through the extensive mud flat area drain into the channel. The surroundings of the channel undergo a longterm process of slow continuous sedimentation by fine sediments.
Various bed samples (core samples: diameter 40 mm; length= 100 mm) have been taken during conditions without any mud layer deposits on the fine sandy channel bed. The bed samples were analysed using sieve analysis and settling tests to determine the sediment composition of the bed. The settling tests consisted of the determination of the settling velocities of the sample sediments which were converted to an equivalent grain diameter using the settling velocity formula of Stokes. The percentage of organic materials was found to be relatively small (<2%). Halfway the channel length, the bed consists of fine sand with d_{50} of about 100 to 150 µm in the middle of the cross-section. The percentage of fines < 63 µm varies between 5% and 25%, mostly in the corners (east, west) of the cross-sections. The channel bed is slightly less fine near the entrance of the channel.
Measurements of tidal water levels (pressure), flow velocities (electromagnetic) and sediment concentrations (mechanical and optical) have been taken at three stations (at 600 m, 1000 m and 1500 m

from the gate station). The mud concentration measurements are largely based on the analysis of water-sediment samples taken by a pump at 0.4 m above the local bed.
The critical flow velocity for particle/surface erosion of sandy channel bed is estimated to be about 0.4 to 0.5 m/s or a critical stress of about 0.25 to 0.30 N/m^2 for the sand fraction.
The critical flow velocity for particle/surface erosion of fresh mud from the channel bed is about 0.2 to 0.3 m/s resulting a critical bed-shear stress of 0.15 to 0.2 N/m^2 (no biological effects).

Deltares (2016) has reported field data of mud concentrations and bed samples in the Dutch Holwerd subtidal channel, which is the sailing route of the ferry between the mainland and the island of Ameland in the Dutch Wadden Sea. The tidal channel has a depth of 4 m below mean sea level and is dredged regularly to maintain the navigation depth. The channel bed is muddy-sandy (45% mud < 63 μm) in the middle of the cross-section and very muddy (75% mud < 63 μm) at the corners of the channel cross-section. The measured suspended sediment samples mainly consist of silty and clayey materials; the sand content is less than 10%.
The critical flow velocity for erosion of sand from the channel bed is estimated to be about 0.5 to 0.6 m/s or a critical stress of about 0.3 to 0.35 N/m^2 for sand.
The critical flow velocity for erosion of mud from the channel bed is about 0.3 to 0.4 m/s resulting a critical bed-shear stress of 0.2 to 0.25 N/m^2 (no biological effects).

2.4 Synthesis of results; soft to firm mud-sand beds

Critical bed-shear stress and velocity
Table 2.4.1 summarizes the available data of critical bed-shear stress values for particle and surface erosion of mud-sand mixtures without biogenic effects. The most influencial parameters are the percentage of fines (<63 μm) and the dry bulk density of the mud-sand mixture. The precise type of erosion (particle or surface erosion) is not the same for all data. Most data are based on visual observations of particle erosion. Some data are based on definitions of erosion related to sudden changes of measured concentrations or pickup rates (plots of concentration/pickup rate against bed-shear stress).
Figure 2.4.1 shows the measured results of **Table 2.4.1**. The vertical error bars represent the scatter range of the measured values of **Table 2.4.1**. Some data of **Table 2.2.1** for pure mud beds are also shown.
Two consolidation stages are distinguished: firmly consolidated with dry mixture density > 800 kg/m^3 (symbols: closed circles) and weakly consolidated with dry mixture density values < 500 kg/m^3 (symbols:open triangles and crosses).
The critical bed-shear for particle/surface erosion of a weakly consolidated pure mud bed with a dry density < 400 kg/m^3 is of the order of 0.2±0.1 N/m^2. The critical bed-shear for particle/surface erosion of a firmly consolidated mud bed with a dry bulk density >800 kg/m^3 is of the order of 1±0.5 N/m^2. The critical bed-shear stress decreases to about 0.4 N/m^2 for $p_{fines} \cong 0.3$. For $p_{fines} < 0.3$, the dry density of the mud-sand mixture is relatively high > 800 kg/m^3 and the critical bed-shear stress of the sand fraction is dominant with critical bed-shear stress values in the range of 0.2 to 0.4 N/m^2. It is most logical to assume that the sand particles are more difficult to erode due to the binding effects of the mud particles surrounding the sand particles. Mud particles will be washed out, once sand particles are eroded. Hence, the critical stresses of both the sand and mud fraction are almost the same. Most likely, the critical stress of the mud fraction will be slightly smaller, as the skin layer of mud around the sand particles needs to be broken first.
In the case of a high mud percentage ($p_{fines}>0.7$), the bulk density of the mud-sand mixture is generally relatively low (dry density<400 kg/m^3) in dynamic subtidal conditions with significant reworking of the bed surface (tidal channels). High bulk densities (> 800 kg/m^3) do occur mostly in quiescent tidal environments where subtidal deposition is dominant (tidal channels with very low velocities <0.3 m/s). Intermediate bulk densities (dry density of 400-800 kg/m^3) generally occur at intertidal mud-sand flats. The critical bed-shear stress of the mud fraction is dominant for $p_{fines}>0.7$. In that case, the sand particles are scattered throughout the mud fraction

and surrounded by many layers of mud particles and are thus much more difficult to erode than the mud particles. Hence, the critical bed-shear stress of the sand fraction is most likely much larger than that of the mud fraction.

Tentative equations for the critical bed-shear stress for particle erosion are:

$$\tau_{crp,finefraction} = \phi_{cohesive}\ \tau_{cr,fine,o} = (1+p_{fines})^{\beta}\ \tau_{crp,silt.o} \quad \text{for particles} < 63\ \mu m \text{ (fine range)} \quad (2.4.1)$$

$$\tau_{crp,sandfraction} = \phi_{cohesive}\ \tau_{cr,sand,o} = (1+p_{fines})^{\beta}\ \tau_{crp,sand,o} \quad \text{for particles} \geq 63\ \mu m \text{ (sand range)} \quad (2.4.2)$$

with:

$\tau_{crp,silt,o}$; $\tau_{crp,sand,o}$; = critical bed-shear stress for particle erosion without cohesive effects($\tau_{crp,silt,o} \cong 0.1$ N/m^2 for silt and $\tau_{crp,sand.o} \cong 0.2$ N/m^2 for fine sand);

$\beta = (1 + \rho_{dry,mixture}/\rho_{dry,max})^{\alpha}$

$\rho_{dry,mixture} = (1-p_{fines})\ \rho_{dry,sand} + p_{fines}\ \rho_{dry,fines}$; $\rho_{dry,max}$ = maximum dry bulk density of mud-sand mixture ($\cong$ 1600 kg/m^3),

p_{fines}= percentage of fines < 63 μm of the bed layer,

$\rho_{dry,sand}$ = dry bulk density of sand ($\cong$ 1600 kg/m^3),

$\rho_{dry,fines}$= dry bulk density of mud ($\cong$ 200 kg/m^3 for soft mud up to 1200 kg/m^3 for firm mud bed);

α= empirical coefficient ($\cong$2).

The wet density ($\rho_{dry,wet}$) can be determined most easily by the measured wet mass and volume of the sample. The dry density follows from: $\rho_{dry,mix}=[\rho_{dry,wet}-\rho_w][\rho_s/(\rho_s-\rho_w)]$ with ρ_s= sediment density ($\cong$2650 kg/m^3) and ρ_w=sea water density ($\cong$1020 kg/m^3).

If $\rho_{dry,mix}$ and p_{fines} (wet sieving using mesh of 63 μm) are known, the $\rho_{dry,mud}$ can be computed as:

$\rho_{dry,mud}=[\rho_{dry,mix}-(1-p_{fines})\rho_{dry,sand}]/p_{fines}$.

Equations (2.4.1) and (2.4.2) are shown in **Figure 2.4.1** for a dry mud density of 300 kg/m^3 in the case of weakly consolidated mud and 1000 kg/m^3 in the case of firmly consolidated mud. The trends of the data are reasonably well represented for $\alpha \cong 2$.

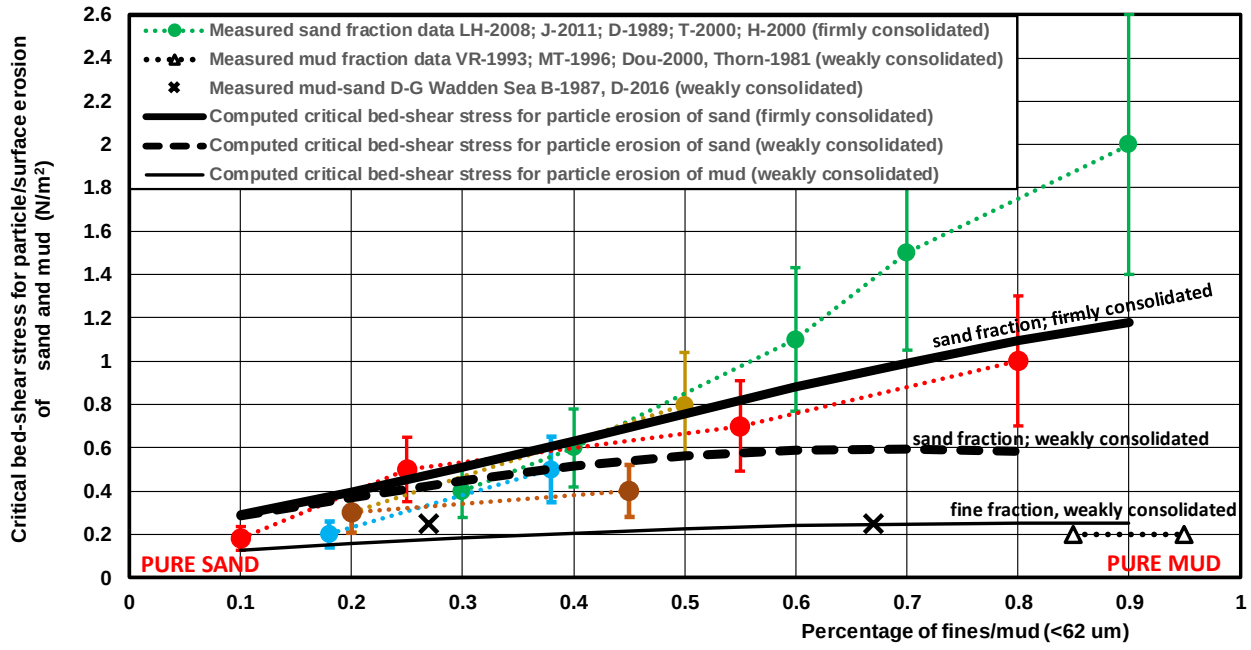

LH= Le Hir; J=Jacobs; D=Deltares; T=Tolhurst; H=Houwing; VR=Van Rijn; MT= Mitchener-Torfs; B= Bauamt

Figure 2.4.1 *Critical bed-shear stress for particle/surface erosion as function of percentage of fines and dry bulk density of the mixture*

Type of mud-sand mixture	Percentage mud (< 63 μm)	Mean sediment size d_{50} (μm)	Dry bulk density top layer (kg/m³)	Critical bed-shear stress for particle (p.e.) and surface erosion (s.e.) of sand and mud fraction (N/m²)
Laboratory flume (Jacobs 2011)	10%	100-150	>1800	0.18±0.04 (p.e./s.e.)
Laboratory flume (Jacobs 2011)	25%	80-100	>1800	0.5±0.15 (p.e./s.e.)
Laboratory flume (Jacobs 2011)	55%	60-80	>1800	0.7±0.3 (p.e./s.e.)
Laboratory flume (Jacobs 2011)	80%	30-60	>1800	1±0.4 (p.e./s.e.)
Lab and field (Le Hir et al. 2008)	20%	<140	> 1500	0.25±0.05 (p.e./s.e.)
Lab and field (Le Hir et al. 2008)	30%	<140	> 1500	0.4±0.1 (p.e./s.e.)
Lab and field (Le Hir et al. 2008)	40%	<140	> 1500	0.6±0.15 (p.e./s.e.)
Lab and field (Le Hir et al. 2008)	60%	<140	> 1500	1.1±0.3 (p.e./s.e.)
Lab and field (Le Hir et al. 2008)	70%	<140	> 1500	1.5±0.4 (p.e./s.e.)
Lab and field (Le Hir et al. 2008)	90%	<140	> 1500	2.0±0.5 (p.e./s.e.)
Lab and field (Mitchener-Torfs 1996)	>70%	<63	400	0.2±0.1 (p.e./s.e.)
Lab and field (Mitchener-Torfs 1996)	40%	<100	800	0.6±0.3 (p.e./s.e.)
Lab and field (Mitchener-Torfs 1996)	30%	<100	1000	1.0±0.4 (p.e./s.e.)
Dutch Wadden Sea intertidal flats (Houwing	<10%	100-150	>1000	0.1-0.2 (p.e.)
Dutch Wadden Sea intertidal flats (Houwing 2000)	15%-20%	100-150	>1000	0.1-0.2 (p.e.)
Dutch Wadden Sea intertidal flats (Houwing 2000)	35%	50-100	>1000	>0.5 (p.e.)
Dutch Wadden Sea subtidal channel Holwerd (Deltares 2016)	70%	20-50	300-500	0.2-0.25 mud fraction 0.3-0.35 sand fraction (surface erosion)
Dutch North Sea bed (subtidal) (Deltares/Delft Hydraulics 1989)	0-30%	100-150	>800	0.2-0.4 (p.e.)
Dutch North Sea bed (subtidal) (Deltares/Delft Hydraulics 1989)	50%	50-100	>800	0.6-1.0 (p.e.)
German Wadden Sea intertidal flats (Tolhurst et al. 2000)	15%-30%	100-150	> 1000	0.2-0.5 (p.e.)
German Wadden Sea intertidal flats (Tolhurst et al. 200)	40%-50%	50-100	>800	0.2-0.5 (p.e.)
German Wadden Sea subtidal channel Nessmersiel (Bauamt 1987)	5%-30%	60-100	300-500	0.15-0.2 mud fraction 0.25-0.3 sand fraction (surface erosion)
Lunenburg basin (subtidal), Nova Scotia, Canada (Sutherland et al. 1998)	20%-30%	30-40	<400	0.05-0.15 (p.e.)
Minas basin (subtidal), Bay of Fundy, Canada (Amos et al. 1992)	65%	20-30	>1000	0.5-1.5 (p.e.)
Tidal fraser river (intertidal), Canada (Amos et al. 1997)	65%-90%	10-20	<400	0.15-0.5 (p.e.)
Hudson Bay (subtidal), Canada (Amos et al. 1996)	40%-50%	40-60	>1000	> 3.5 (p.e)

p.e.= particle erosion; s.e.= surface erosion

Table 2.4.1 *Critical bed-shear stress for erosion of mud-sand mixtures without biogenic effects*

Figure 2.4.2 shows the critical bed-shear stress for surface erosion as function of the dry density of the top layer based on the HTS (HANZE Technical School)-data presented by Van Rijn (2020); four ranges related to the percentage of fines (< 63 μm) are distinguished: p_{fines}<15%, 15%-30%, 30%-60% and 60%-90%. The critical bed-shear stress at the moment of bed failure (mass erosion) is also shown. For example, a mud bed with pfines=25% and a dry density of 800 kg/m³ has a critical stress of about 0.4 N/m² for surface erosion and about 0.8 N/m² for mass erosion.
It is noted that the critical bed-shear stress for surface erosion (generation of grooves) is much larger (factor 1.5 tot 2) than the critical stress for particle/floc erosion of fine fraction. Comparison of the data related to artificial mud-sand beds and in-situ mud-sand beds shows no major differences. The critical bed-shear stress for surface erosion is in the range of 0.4 to 0.8 N/m^2 for both type of beds. Mass erosion occurs for bed-shear stresses > 1.2 N/m^2. The presence of exposed shells leads to somewhat smaller critical stresses as more turbulence is generated close to the surrounding bed surface.
Many data from other sites with low-density mud beds in the range of 200 to 400 kg/m^3 (Thorn 1981; Van Rijn 1993; Mitchener and Torfs, 1996; Dou 2000, Van et al. 2012) are in the same range as the present HTS-data of N-mud and D-mud. Mitchener and Torfs (1996) reported relatively high critical stresses of about 1 N/m^2 for Scheldt mud with p_{fines} in the range of 5% to 15%, whereas in the present HTS-flume tests the critical bed-shear is a factor of 2 smaller for about the same conditions.
The critical bed-shear stresses based on the flume tests of Kothyari and Jain (2008) for highly conslidated mud-sand-gravel beds are in the range of 1 to 2.5 N/m^2, whereas the present HTS-data are in the range of 0.5 to 1 N/m^2 (surface erosion) and 1 to 1.5 N/m^2 (mass erosion) for highly consolidated beds. Most likely, this is caused by the relatively high percentage of clay used by Kothyari and Jain (2008).
Discrepancies between various data sets are most likely related to the sediment composition of the mixtures(percentage of clay) and the various definitions of particle/surface/mass erosion applied. For example, the artificial mixtures used by Kothyari and Jain (2008) did not have an appreciable silt fraction (8 to 63 μm); only very fine clay was used enhancing the cohesive effects.
The following phenomena related to surface and mass erosion can be observed (**Figure 2.4.2**):

- p_{fines}<15%; the bed consists of firmly consolidated sediment materials; dry densities are > 1400 kg/m^3; the mud particles are washed out when the sand particles are eroded; critical shear stress is in the range of 0.15-0.25 N/m^2;
- p_{fines}=15%-30%; the bed consists of firmly consolidated sediment materials; dry densities are > 800 kg/m^3; the critical shear stress increases slightly with the dry bulk density; the critical shear stress for mass erosion (small grooves and craters) is much higher (factor 2 to 2.5) than that for surface erosion;
- p_{fines}=30%-60%; the bed consists of soft muddy materials (400-800 kg/m^3) with clear traces of fine sand; the critical shear stress increases moderately with the dry bulk density; the critical shear stress for mass erosion is much higher (factor 2) than that for surface erosion;
- p_{fines}=60%-90%: the bed consists of very soft muddy materials; the critical shear stress increases strongly with the dry bulk density; the critical shear stress for mass erosion is higher (factor 1.5 to 2) than that for surface erosion.

Surface and mass erosion of weak to medium consolidated mud-sand beds (dry density < 800 kg/m^3) can be crudely related to the critical stress for particle erosion: $\tau_{cr,se} \cong 1.5\ \tau_{cr,pef}$ and $\tau_{cr,mass} \cong 3\ \tau_{cr,pef}$.
The critical depth-mean flow velocity for surface and mass erosion can be determined from the Chézy-equation. Using: $\tau_{cr}=\rho g\ u_{cr}^2/C^2$, it follows that $u_{cr} \cong C\ (\tau_{cr}/(\rho g))^{0.5}$, with u_{cr}= depth-mean velocity at critical conditions, C= Chézy-coefficient (about 80 to 100 m$^{0.5}$/s for muddy field sites).
Figure 2.4.3 shows the critical depth-mean velocity for surface erosion and mass erosion of the mud fraction based on the data of Figure 2.4.2 and C=90 m$^{0.5}$/s and is valid for depths between 1 and 5 m. The critical velocities are in the range of 0.5 to 1.5 m/s depending on the percentage of fines < 63 μm and the dry bulk density. The cohesive effects are largest for p_{fines} > 60%. Bisshop (2018) has studied the pickup of fine silt and sand in a recirculating pipeline system. The finest sediment was silt with a mean size of about 50 μm ($p_{fines}\cong$70%;

firmly consolidated bed of about 1500 kg/m^3). Mass erosion with a pickup rate of about 1000 gr/m^2/s did occur for a mean velocity of about 1.7 m/s and a depth of about 0.2 m. The equivalent mean velocity for a depth of > 1 m is about 2 m/s (see Figure 2.4.3).

The data of **Figures 2.4.2** and **2.4.3** can be used to get a better understanding of the erosive behaviour of tidal channels with mud-sand bed mixtures. Three cases are considered:

- Tidal channels with a dynamic bed consisting of low-density mud (weakly consolidated; p_{fines}> 0.7; dry density < 400 kg/m^3) mostly occur in a regime with relatively high velocities (>0.7 m/s) resulting in significant reworking of the bed surface during the tidal cycle. The critical bed-shear for surface erosion for this type of conditions is about 0.2 to 0.4 N/m^2;
- Tidal channels with a bed consisting of high-density mud (firmly consolidated; p_{fines}> 0.7; dry density > 800 kg/m^3) are mostly present in quiescent tidal environments with relatively low velocities (< 0.3 m/s) where the fine sediments can deposit and consolidate. The critical bed-shear for surface erosion for this type of conditions is about 0.8 N/m^2 or larger;
- Tidal channel beds with intermediate bulk densities (dry density of 400-800 kg/m^3) generally occur along the banks in the transition zones to the intertidal mud-sand flats. The critical bed-shear stress of the fine fraction and the sand fraction is in the range of 0.4 to 0.8 N/m^2.

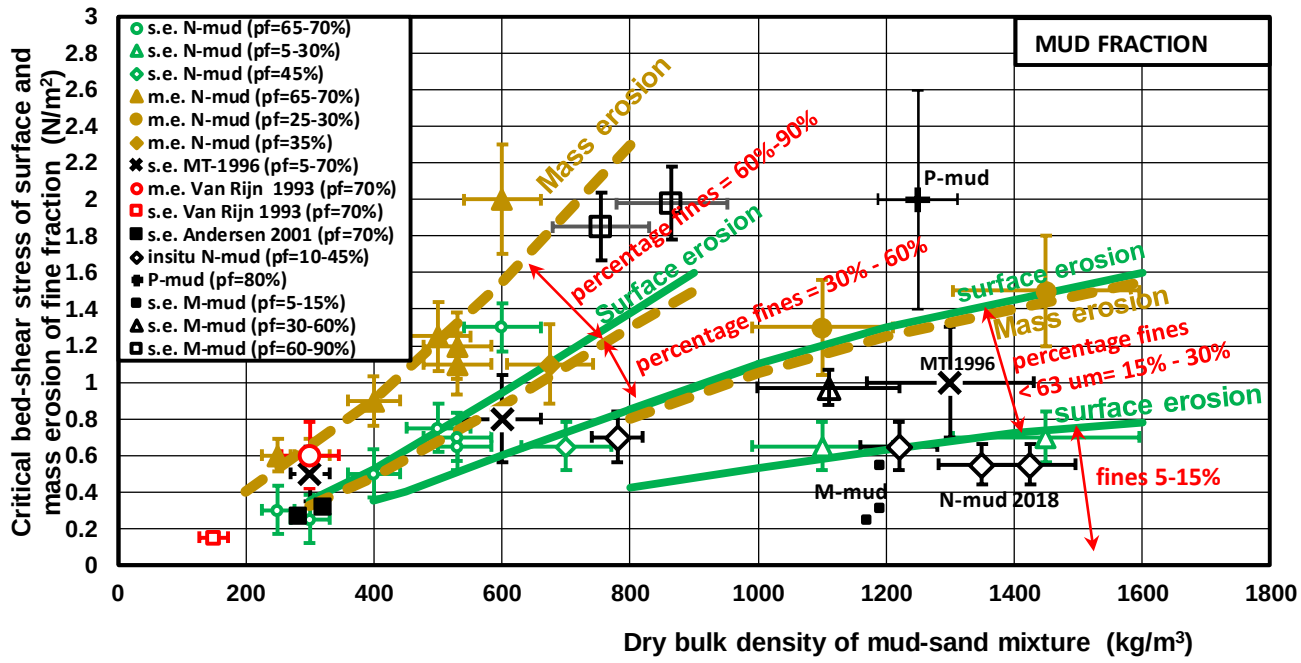

Figure 2.4.2 *Critical bed-shear stress for surface and mass erosion (pf= percentage fines; MT= Mitchener and Torfs; p.e=particle erosion; s.e=surface erosion; m.e= mass erosion; N-mud= mud from Noordpolderzijl, Netherlands; P-mud= mud from Payra, Bangladesh; M-mud= mud from Mississippi, USA, Wu et al., 2017)*

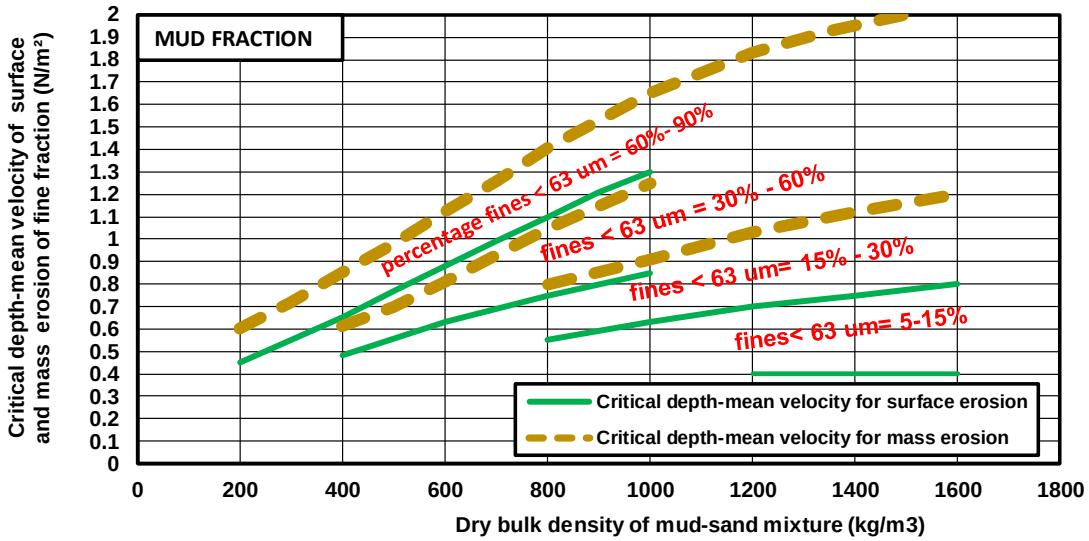

Figure 2.4.3 *Critical depth-mean velocity for surface and mass erosion; water depths of 1 to 5 m; C= 90 $m^{0.5}/s$*

Erosion rates

At the bed, two simultaneous processes do occur: erosion and deposition. A rough indication of the erosion rates of mud-sand mixtures is given in **Figure 2.4.4**. For clearness the measured values are omitted. The erosion rate increases for increasing bed-shear stress ($E \sim \tau_b^2$) and decreases strongly for increasing dry density (400, 600, 700, 800 and > 1000 kg/m³). The erosion rate of fine cohesionless sand of 63 μm measured in a high-velocity pipeline circuit is also shown (Van Rijn et al. 2019). Strong damping of turbulence at high bed-shear stress was observed for cohesionless fine sand resulting in a less steep increase of the erosion rate of fine sand. The erosion rate of mixtures of clay-silt-sand is smaller than that of fine cohesionless sand due to the cohesive effects of the very fine clay fraction reducing the erosion rate of cohesive mixtures.

The deposition flux is defined as: $D=c_b w_s$ with c_b= near-bed concentration of fines (range of 10 to 100 kg/m³) and w_s= settling velocity near the bed (range of 0.5 to 1 mm/s). Using these values, an estimate of the deposition flux is 5 to 100 gram/m²/s, which is of the same order of magnitude as the erosion rate. Hence, fairly stable channel beds are possible in muddy conditions.

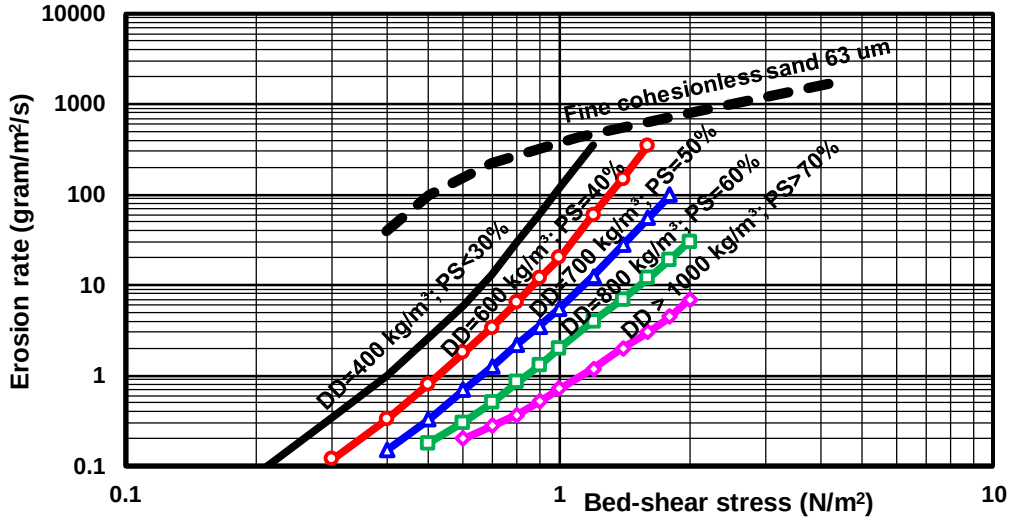

Figure 2.4.4 *Erosion rates of mud-sand mixtures (DD=dry density; PS= percentage of sand)*

3. Effect of biogenetic factors

3.1 Intertidal mud-sand flats

The presence of organic material has a great effect on the erosional behaviour of a mud-sand bed. The bed surface can become cemented due to slimes produced by diatoms and bacteria. Bioturbation can be the cause of a reduction in erosion resistance of the bed surface. The presence of organic material may also have a great effect on the erosional behaviour of a mud-sand bed.
The critical shear stress for motion and suspension (erosion) is highly influenced by biotic processes.
Benthic processes are caused by the community of organisms living on, in or near the sea bed.
Two main effects are present:

- microphytobenthos; micro algae populations live/grow as patchy biofilms in the topmost 3 mm of the seabed after periods of sunny and calm weather; diatoms are a group of single celled algae that are engaged in a silica cell wall; diatoms produce extracellular colloidal carbohydrates (slimes) and extracellular polymeric substances (EPS) creating bonds between the bed-particles resulting in higher crtical stresses;
- macrozoobenthos; benthic animals large enough to be seen by eye; small-scale animals (snails, cockles) may also affect the erodibility of fine-grained sediments; both directly due to bioturbation and fecal pelletisation of the bed and indirectly due to grazing on diatoms.

Due to the strong temporal and spatial variability of the stock of benthic diatoms, large spatial and temporal variations in the erodibility of intertidal mudflats do occur.These effects can be best studied by using in-situ instruments.

Amos et al. (1992) have studied the erodibility of fine-grained sediments in Minas basin within the Bay of Fundy (Canada) using the benthic annular flume, Sea Carousel.
Minas basin: bed of 30% to 40% sand, 40% to 60% silt and 10% to 20% clay and wet bulk density of 1800 kg/m^3. Surface sediments are biologically active (diatoms) and the pelletization process is high. Each winter, ice removes the upper 0.10 m of the mud bed surface at Minas basin. The surface layer is regenerated through tidal sedimentation each spring. Deposition occurs at concentrations below 50 mg/l. The repetitive measurements of sediment erodibility were made during July and August, 1989 and July, 1990 at three stations along a transect of a littoral mudflat in the Southern Bight of Minas Basin Minas This basin is strongly macro- tidal (semi-diurnal mean tides of 11.5 m tidal range) and is subject to intermediate wave activity and ice cover.
Surface erosion (Type I-eroison) occurred at imposed bed stresses between 0.5 and 1.5 N/m^2 at Minas basin and between 1 and 2.5 N/m^2 after a bloom of diatom production, see **Table 3.1**. Surface erosion erosion occurred only in the uppermost 0.5 mm of the bed. At deeper layers Type II-erosion was dominant. Type II-erosion (mass erosion) was constant with time was independent of changes in bulk bed shear strength with depth.

Bed type	Percentage mud (<63 μm)	Mean size d_{50} (μm)	Dry bulk density (kg/m^3)	Chlorophyll content	Critical shear stress for surface eosion (N/m^2)
Minas basin; Bay of Fundy, Canada	65%	30-40	> 1000	not measured	0.5-1.5

Table 3.1 *Critical bed-shear for erosion at sand-mudflat, Minas basin, Bay of Fundy, Canada*

Andersen et al. (2010) have used the in-situ instrument EROMES. The study site is a mixed mudflat situated on ''Dornumer Nacken'' in the tidal basin behind the barrier islands Baltrum and Langeoog in the East Frisian part of the German Wadden Sea Area in the southern North Sea. The basin is mesotidal with a tidal range of approximately 2.6 m. The basin consists largely of intertidal sand flats and mixed mudflats. The fine sediment fraction < 63 μm is in the range of 30% to 40% (mud content). The average inundation period during each tidal cycle is 7 hours during calm weather conditions and maximum tidal current velocities are about 25 cm/s. A hummocky surface was present in June 2002 with alternating crests and pools of a horizontal scale of about 1 m and heights of up to about 5 cm. The crests were lower in September and November (maximum about 2 cm) and bedforms were absent in February and April 2003.
Bed samples were taken by scraping of the topmost 1 mm of the bed and were analysed for grain-size distribution, fecal pellet content, organic content, content of chlorophyll a, water extractable colloidal carbohydrate and extracellular polymeric substances (EPS). Analyses of carbohydrates were only carried out in June and September. Additional samples of the topmost 5 mm of the bed were taken with a suction needle (syringe with diameter 21 mm, five samples pooled into one sample) and analysed for dry bulk density. Grain-size analyses were carried out by use of a Malvern Mastersizer/E laser-sizer after careful dispersion (deflocculation) and ultrasonic treatment prior to analysis. Fecal pellets were abundant at the site and the pellet contents of the bed material and calibration samples for the OBS-sensor were determined by gentle wet-sieving of a sub-sample at 63 μm and examination of the retained material under microscope in order to estimate the fecal pellet content in this material. The retained material was subsequently given an ultrasonic treatment and wetsieved at 63 μm again in order to separate fecal pellet material and sand and shell-fragments. Organic contents were determined. Chl a contents were determined after extraction in 90% acetone by high performance liquid chromatography and by spectrometry. The contents of colloidal (water extractable) carbohydrate and EPS were quantified using the phenol-sulphuric spectrometric assay/procedure.
The sediment from each erosion core was sieved at 1 mm and the macrozoobenthos were described and counted (range of 100 tot 3000 individuals per m^2).
The erosion experiments were carried out using a portable EROMES erosion apparatus. Additional experiments were carried out using the original laboratory version of the same instrument. Undisturbed sediment cores were
brought ashore and analysed in the laboratory EROMES.
Basically, the EROMES erosion instrument consists of a 100 mm diameter perspex tube that is pushed into the undisturbed bed sediment. The tube is gently filled with local seawater and the eroding unit is placed on top of the tube. This eroding unit consists of a propeller that generates a primarily tangential flow and bed-shear stresses. An OBS-sensor inside the tube monitors the changing suspended sediment concentration. The propeller revolutions are transferred to bed shear stress by use of a calibration based on the onset of erosion of quartz sands with known critical erosion shear stress. During each erosion experiment, the bed shear stress was increased in steps of 0.1 N/m^2 every 2 minutes from 0.1 to 1 N/m^2.
The erosion thresholds were determined by use of plots of erosion rates versus applied bed stress. A linear fit was made through the data points in the region of the onset of erosion and the threshold was determined as the bed shear stress at the intercept of this line with a critical erosion rate; the erosion rate above which significant erosion of the sediment surface starts to take place. A critical erosion rate of 0.01 $g/m^2/s$ was used which corresponds to the erosion of the least stable material at the surface (low-density flocs and bioaggregates). Samples for the calibration of the OBS-sensor were withdrawn from the tube during each experiment and filtered. The aggregation and settling velocity of the eroded material were analysed as part of the erosion experiments by monitoring the change in suspended concentration as the propeller was turned off after the last step and the suspended material was allowed to settle. In order to make the data directly comparable (compensate for the changing viscosity of the water with changing temperature), the settling velocities were converted to equivalent settling diameters by use of Stokes' law. The actual diameter of the aggregates is larger, often much larger, due to the lower density and irregular shape of the aggregates.

The surface sediments at the site were a mixture of very finegrained sand and mud and the grain-size distributions of the bed material were bi-modal and showed that the surface material consisted of well-sorted sand with an average grain-size of about 105 μm and poorly sorted silt and clay with a mode at about 15 μm.
The mud content of the surface material was about 35% and showed no significant temporal variation but a decrease with depth was observed, reaching about 15% mud at 20 cm depth.

The erosion thresholds for the sediments generally varied between 0.2 and 0.6 N/m^2 (**Table 3.2**) but significantly higher thresholds (up to 1.8 N/m^2) were observed in September and April. Similarly, significantly higher contents of chlorophyll a were observed in September and April and lower contents in the rest of the study period.

Bed type	**Percentage mud (<63 μm)**	**Mean size d_{50} (μm)**	**Dry bulk density (kg/m^3)**	**Chlorophyll content (mg/m^2 ≅ μg/g)**	**Critical shear stress for surface eosion (N/m^2)**
Dornumer Nacken'' East Frisian German Wadden Sea	35%	15-100	700-1120	<10	0.2-0.3
				10-20	0.2-0.6
				20-40	0.4-1
				40-80	1-2

(1 mg/m^2 in layer of 1 mm thick ≅ 1mg/kg ≅ 0.001 mg/g ≅ 1 μg/g)
Table 3.2 *Critical bed-shear for erosion at sand-mudflat, East Frisian Wadden Sea, Germany*

Figure 3.1 shows a comparison of the average suspended concentration data from the experiments in September 2002 and February 2003.

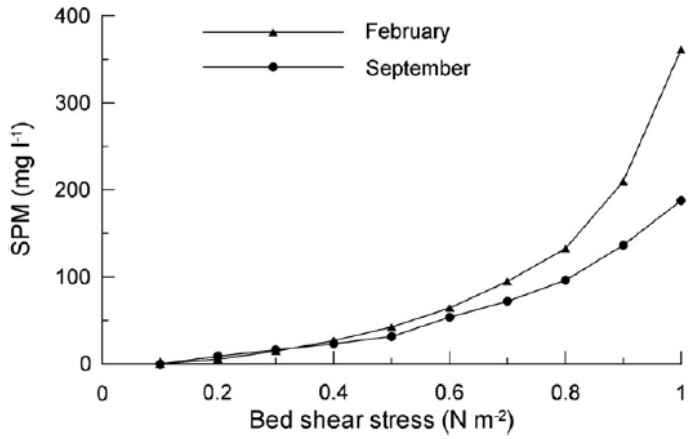

Figure 3.1 *Suspended concentrations in September 2002 and February 2003*

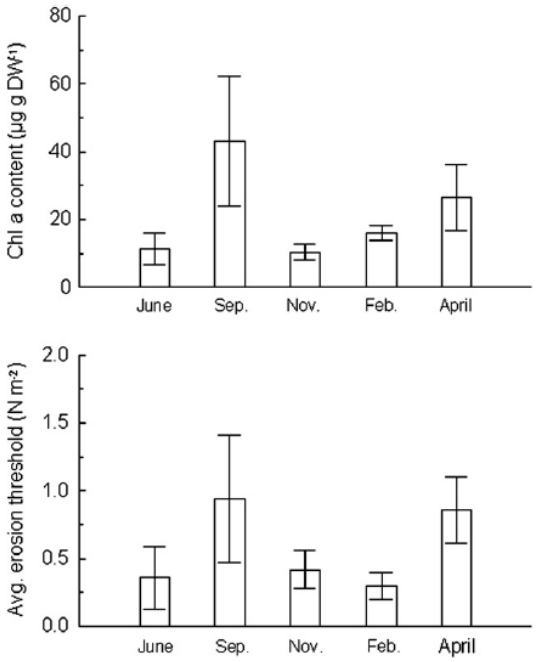

Figure 3.2 *Temporal variation of critical stress and chl a-content, East Frisian Wadden Sea, Germany*

Figure 3.2 shows a plot of the temporal variation of the chl a content and erosion threshold. Colloidal carbohydrates and EPS were only measured in June and September and much larger values were observed in September.
The dry bulk density of the sediment varied between 700 and 1150 kg/m^3 and organic content between 1.3% and 3.6%. Neither macrofauna densities, dry bulk density, fecal pellet content or organic content showed significant temporal variations.
No significant differences were observed in June but the chlorophyll a contents were higher on crests than in troughs in September. In November, erosion thresholds were higher on crests than in troughs. Bedforms were absent in February and April 2003.
The erosion thresholds were especially well correlated to the contents of chlorophyll a, colloidal carbohydrates and EPS, see **Figures 3.3** and **3.4**. The site was primarily controlled by microphytobenthos, which may vary considerably temporally and spatially. Its effect is smaller in autumn and winter due to lower light-intensity and higher wave action. Drying will also contribute to differences in erodibility during warm periods with high evaporation.

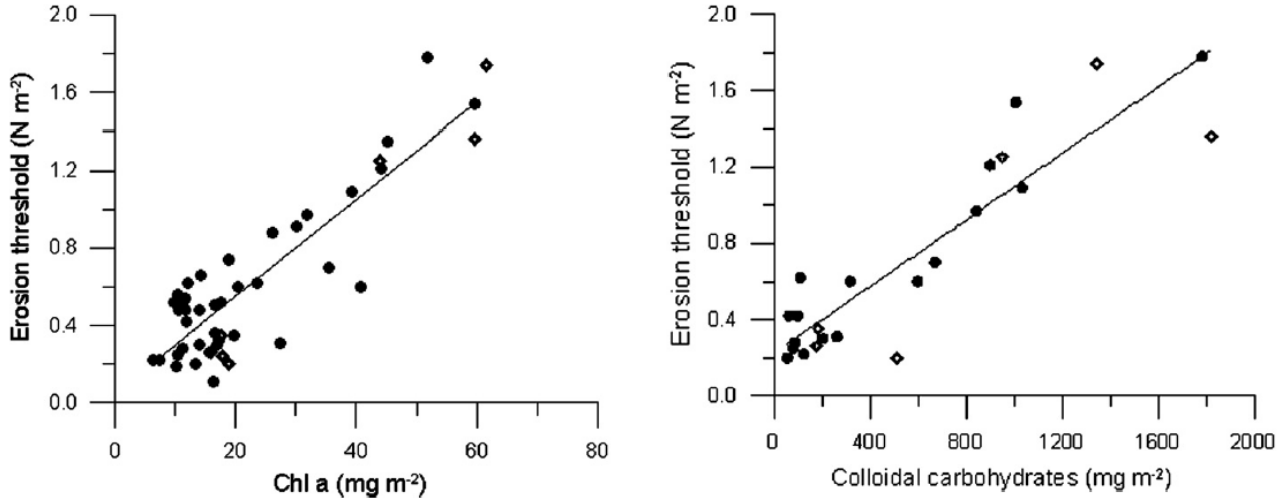

Figure 3.3 *Critical bed-shear stress as function of Chl a-content and colloidal carbohydrates-content (solid circles= in-situ EROMES; diamonds= laboratory EROMES); East Frisian Wadden Sea*

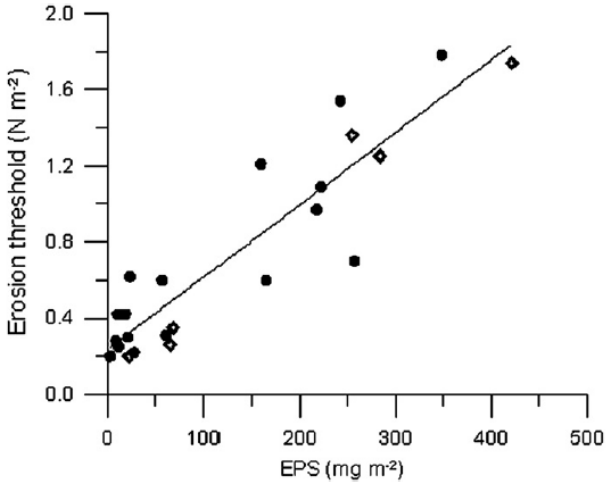

Figure 3.4 *Critical bed-shear stress as function of EPS-content; East Frisian Wadden Sea, Germany (solid circles= in-situ EROMES; diamonds= laboratory EROMES)*

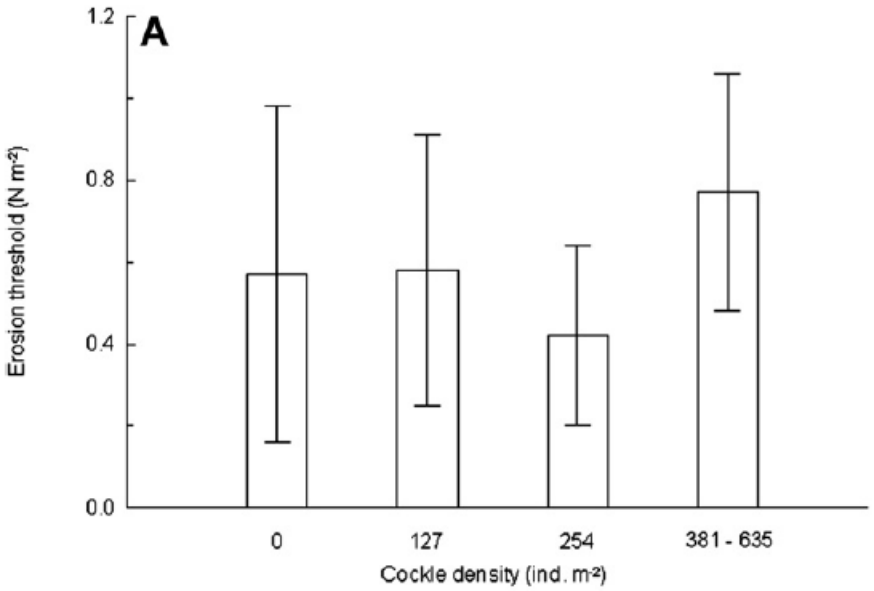

Figure 3.5 *Critical bed-shear stress as function of cockle density; East Frisian Wadden Sea, Germany*

In the order of 80% of the variance in the erosion thresholds can be explained by these indirect measures of microphytobenthic stock. The data from the portable and the laboratory-version of the EROMES are plotted separately in **Figures 3.3** and **3.4**. A test of the influence of erosion-method using a multiple linear regression showed no significant difference. There was no correlation between the erodibility of individual sediment cores and the density of the cockles in the cores (**Figure 3.5**). The presence of cockles may lead to increased erodibility of the sediments caused by burrowing activity (rougher surface) and the exhalent jets from the cockle's siphons.
A biostabilisation index can be calculated as the ratio of the erosion thresholds with and without biological influence. If the hypothetical (and unrealistic) case of complete absence of colloidal carbohydrates and/or EPS is considered, an expected erosion threshold of about 0.2 N/m^2 can be found based on the linear fits in Figures 3.3 and 3.4. Using this value as a best estimate of the erosion threshold at abiotic conditions a stabilisation index of 4.7 is found in September and 4.3 in April. The content of sand in suspension was still lower than the bed material.

Andersen (2001) has studied the erodibility of two microtidal mudflats in the Danish Wadden Sea over a year at monthly intervals using the in-situ EROMES erosion instrument. One site was dominated by macrofauna, whereas the other was only sparsely inhabited by macrofauna with the temporary formation of diatom biofilms. The sites are situated in the microtidal Lister Dyb tidal area (Kongsmark) and the microtidal Ho Bugt, Gradyb tidal area (Kjelst), both in the Danish part of the European Wadden Sea area.
The tidal range in the Lister Dyb tidal area is 1.8 m compared to a tidal range of 1.6 m in Ho Bugt. The tidal flats in both tidal areas are generally sandy but the study sites are situated in sinks for fine-grained material and the mean grain-size is approximately 10 μm at both sites. About 80% of the dispersed material show equivalent settling diameters finer than 2 μm and the organic content of the bed material varies generally between 8 and 15%. These mudflats are generally very flat with no distinct bedforms or channels and the relief is typically 1 to 2 cm and the slope about 1‰. Small ripples (height 2 mm and length 50 mm) are often found despite the very fine-grained texture of the primary grains and this shows that the bed-material is highly aggregated. A hummocky surface is occasionally formed when the mudflats are undergoing erosion, especially in areas of patchy biofilms.

The Kongsmark site has a relatively large macro-faunal population. Fecal pellets make up a large portion of the bed material at Kongsmark during most seasons and typical lengths and densities of these pellets are 0.1 to 0.3 mm and 1030 to 1140 kg/m^3.
The macro faunal population at the Kjelst site is smaller due to the much more variable salinities**.**
The erosion device used for the determination of erosion threshold and erosion rate was a portable version of the German EROMES apparatus, originally developed by the GKSS research centre. The portable EROMES version consists of 10 cm diameter perspex tubes which are pushed into the undisturbed bed sediment. The tubes are gently filled with local sea-water and the eroding unit is placed on top of the tubes. This eroding unit consists of a propeller which generates bed shear stresses and an OBS-sensor which monitors the changing suspended sediment concentration (SSC). The propeller revolutions have been converted to bed shear stress by use of a calibration based on erosion of quartz sands with known critical erosion shear stress. The OBS-sensor was calibrated by filtering of 100 ml-subsamples withdrawn from the system with a pipette during the erosion experiments.
It was found that a critical value of 0.1 g/m^2/s was suitable to discriminate between the erosion of the fluffy top-layer and the erosion of the bed itself. This value corresponds to 360 g/m^2/hr or 0.5 to 1 mm/h for the dry bulk densities found for the bed sediments at the sites.
For each erosion experiment two sediment samples were collected. One sample consisted of the surface scrape of the topmost 1 to 2 mm of the bed and was analysed for grain size, fecal pellet content, chlorophyll *a* and phaeopigment. The second sample consisted of five subsamples of the topmost 5 mm of the bed taken with a 20-ml syringe, in total 10 ml. This sample was used for the determination of wet and dry bulk density and water content. Grain size analyses were undertaken on selected samples and carried out by use of both a Sedigraph 5100 (giving the equivalent settling diameter) and a Malvern Mastersizer/E laser-sizer (giving the volume diameter). The chlorophyll *a* content of the surface layer of the bed was used as an indicator of the amount of living diatoms.
The fecal pellet content of the bed material and calibration samples for the OBS-sensor were determined by gentle wet-sieving of a sub-sample at 63 μm and examination of the retained material under microscope in order to estimate the fecal pellet content in this material (generally in the order of 90%). The retained material was subsequently given an ultrasonic treatment for 2 minutes and wet-sieved at 63 μm again in order to retain sand and shell-fragments.

The dry bulk density varied between 200 and 350 kg/m^3 for both sites. Particularly high dry densities with an average of 450 kg/m^3 were measured at the Kongsmark site in December 1999 after a period of weak erosion of the mudflat and deposition of fecal pellets.
The organic content was variable with averages between 7 and 14% and no distinct temporal trends were found.
Fecal pellets were mostly absent at Kjelst but occasionally pellets were found at some stations. At Kongsmark, high contents of fecal pellets (generally about 50 to 60%) were found in the period May to October and low contents (generally 10 to 20%) were found in the months November to March.

For both sites the erosion threshold was significantly correlated with the chl *a* content. For the Kongsmark site, average chlorophyll *a* contents were less than 50 μg/g dry weight for all study periods and the erosion thresholds were generally between 0.2 and 0.5 N/m^2. However, patchy diatom mats were present at the most seaward station during most of the study period and the erosion threshold varied between 0.8 and 1·9 N/m^2 at this station and with chl *a* contents up to 190 μg/g dry weight. For the Kongsmark site a negative correlation was also observed between the fecal pellet content and the erosion threshold.
The chl *a* content at the Kjelst site was much more variable both spatially and temporally and the average content varied between 20 and 180 μg/g for the different study periods. The mean erosion threshold at Kjelst shows more variation than at the Kongsmark site and generally higher values were found with average

thresholds ranging between 0.35 and 1.3 N/m^2. Visible biofilms were found at the mudflat surface during both spring and late summer/early autumn and during these periods erosion thresholds above 2.2 N/m^2.
The erosion thresholds plotted as a function of the fecal pellet content indicates that thresholds are low and fairly constant at high fecal pellet contents whereas both high and low thresholds are found at sites with low fecal pellet contents.

Figure 3.6 shows the temporal variation of the average erosion thresholds and chlorophyll *a* contents for both sites. The chlorophyll *a* contents are fairly low and stable at the Kongsmark site whereas a much larger variation is observed at the Kjelst site. At this site a maximum was observed both in the spring and in the late summer/early autumn. The erosion thresholds follow the variation of the chlorophyll *a* content to some extent with high thresholds at Kjelst in spring and late summer/early winter but also fairly high thresholds in January 2000. The erosion thresholds at Kongsmark slowly decreased from February 1999 to October 1999 and later higher values were found in both December 1999 and March 2000.
The erosion threshold at the Kongsmark site shows dependence on the content of fecal pellets with higher thresholds in the cold seasons when the content of fecal pellets is low and low thresholds in the warmer seasons when contents are high. However, the dependence on fecal pellet content is not very strong and it is probably the varying content of benthic diatoms that is governing the erosion threshold.

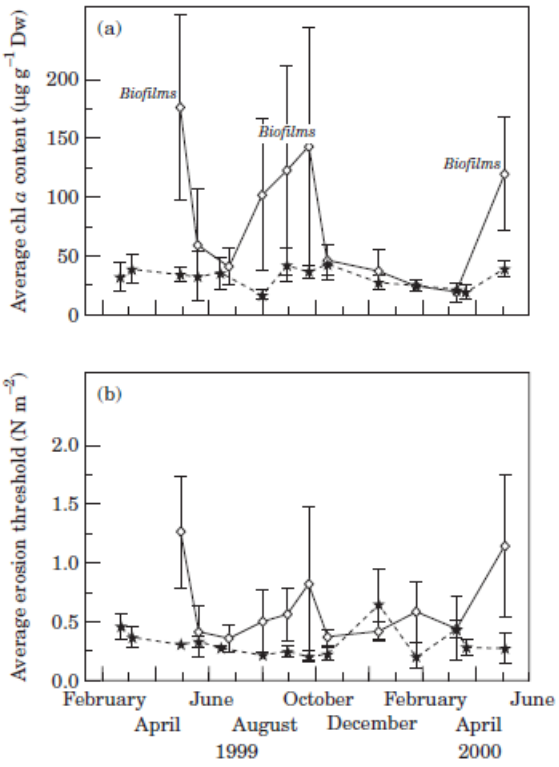

Figure 3.6 *Temporal variation of critical shear stress for erosion (solid symbols= Kongsmark; open symbols= Kjelst)*

The data showed no dependence of either erosion threshold or erosion rate on the dry bulk density of the top bed material.
The study confirms that the erodibility of a mudflat is controlled by both the presence of macrofauna and benthic diatoms and shows that the seasonal variation of erodibility may be very different depending on the biological community structure. Biofilms did not form at sites with high densities of macrofauna and the erodibility of these sites were high due to the high contents of fecal pellets in the bed material.

It must be noted that the results are only applicable to the top few mm of the bed. Deeper layers generally posses higher resistance against erosion and the erosion rate will therefore decline rapidly with time for a given bed shear stress. Consequently, the vertical variation of erosion threshold is needed for a full numerical modelling of the erosional behaviour.

The critical bed-shear stresses of almost pure mud are in the range of 0.2 to 0.4 N/m^2 at both sites, see **Table 3.3**.

Bed type	Percentage mud (<63 μm)	Mean size d_{50} (μm)	Dry bulk density (kg/m^3)	Chlorophyll content (μg/g)	Critical shear stress for surface eosion (N/m^2)
Kongsmark tidal flat, Denmark	80-100%	10	200-400	<50	0.2-0.4
Kjelst tidal flat, Denmark	80-100%	10	200-400	50-150	0.4-0.8

Table 3.3 *Critical bed-shear for erosion at sand-mudflat, tidal flats, Denmark*

3.2 Subtidal mud-sand channel beds

Amos et al. (1996) have studied the erodibility of natural consolidated estuarine sediments using an in-situ sea caroussel flume along a longitudinal transect of Manitounuk Sound, Hudson Bay (Canada). Water depths were in the range of 13 to 45 m and the percentage of organic materials is very small (<1%).
Sea Carousel is a benthic annular flume capable of submarine measurement of seabed stability. The annulus is 2 m in diameter, 0.3 m high and 0.15 m wide. It is equipped with three optical backscatter sensors to monitor water turbidity, an electromagnetic current meter to monitor the flow velocities, a lid rotation sensor and an underwater camera that views the eroding bed through a side window. Flow is induced by rotation of a moveable lid to which are attached eight paddles. Flow velocity is transformed to bed stress based on velocity gradients derived in a series of laboratory tests. Bed stress is increased in the flume in a series of steps of equal duration. Erosion rate (in the range of 1 to 3 g/m^2/s) is evaluated as the increase in suspended mass in the flume with time. Bulk density values are based on gravity cores from each site. The sedimentary column was a highly bioturbated, mottled olive-grey silty clay, with a surface oxidized layer 0.10 m thick. Exceptions were GB13 and GB14 which showed distinct laminations and a surface layer of sandy silt. Deployments lasted about 90 min. Each deployment comprised: (a) a slow descent of the flume to the seabed to minimize seabed disturbance on landing; (b) a still-water interval to allow settling and clearing after deployment and to derive the offsets of the flow meter and the optical backscatter sensors; (c) a period of flow during which the reference current is increased in nine steps up to 0.8 m/s and (d) a still-water period to allow settling of the material eroded in the preceeding interval of flow. Water samples were collected from a port in the side of the Sea Carousel at each speed increment with the aid of a pump. The volume of the hose was flushed and a 500-mL water sample was collected.
Table 3.4 shows the basic data and measured critical stress for erosion of the topmost layer < 1 mm. The data are grouped in three typical groupes of consolidated beds with bulk densities between 1600 and 2000 kg/m^3. The measured critical shear stresses for erosion are smallest for muddy-silty beds with bulk densities of 1700 to 1800 kg/m^3.

Type of bed	Median sediment size (μm)	Percentage clay (%)	Percentage silt (%)	Percentage sand (%)	Wet and dry bulk density (kg/m^3)	Critical bed-shear stress erosion of toplayer < 1 mm (N/m^2)
Muddy-Silty bed (GB3-10,12,15)	3-10	20-65	30-40	5-25	1700-1800 (>1000)	0.7-2
Muddy-Silty bed (GB11,14)	30-40	30-35	15	50-60	1600-2000 (>1000)	3.5-10
Muddy-Sandy bed (GB13)	63	25	15	60	1950 (>1000)	>6

Table 3.4 *Critical bed-shear stress for erosion of consolidated beds in deeper water of Manitounuk Sound, Hudson Bay, Canada*

Sutherland et al. (1998) have used an in-situ carousel flume to study the influence of biofilms on the erodibility of a pure mud bed in a tidal channel (Upper South Cove, Nova Scotia, Canada). Upper South Cove is a shallow coastal embayment situated within Lunenburg Bay, Nova Scotia, located 63 km southwest of Halifax.

Subsamples of the material eroded within the sea carousel were collected by pumping and were analyzed for suspended particulate matter. Undisturbed syringe cores of the seabed at water depths between 3 and 8 m were also collected and analyzed for major physical properties (bulk density, mineralogy, grain size) and organic character (chlorophyll, pheopigment, colloidal carbohydrate, organic content). Sediment cores (syringe cores; diameter=2.6 cm, length= 6 cm) were taken from a Van Veen Grab sample collected at each station located inside the cove. The topmost 1 and 2 mm of a second core collected from each station were analyzed for both chlorophyll and pheopigment concentrations, since the chlorophyll maximum was generally above a depth of 2 mm in the sediment. Slices of each sediment layer were cut in 1-mm depth intervals.

The inner cove region where the samples were taken, is a region of net deposition of fine sediments.

Sediment in the inner cove is characterized by unconsolidated muds. The sediment is highly pelletized with an organic content of about 20% and surface porosities of up to 87%. The average current in the cove is 0.12 m/s. Resuspension of fine material occurs at peak flows of 0.3 to 0.6 m/s during flood tide. Observations made by Scuba in the cove reveal the occurrence of gel-type muds.

Seven stations were chosen along a transect extending over the inner half of Upper South Cove. The erodibility of the sediment at these stations was determined by use of the sea carousel from 16 to 19 October 1993.

The sea carousel has a diameter of 2 m, an annulus width of 0.15 m and a height of 0.30 m. The flow is driven by a movable lid with eight small paddles. A skirt is situated on the outer wall of the annulus and standardizes penetration of the flume into the seabed. Optical backscatter sensors were located inside (0.03 and 0.18 m above the skirt) and outside the annulus to measure ambient and resuspended solids. A window was situated in the inner flume wall, through which an underwater videocamera recorded erosion of the seabed. Longitudinal and vertical components of flow within the annulus were recorded with a Marsh-McBirney electromagnetic current meter.

Figure 3.7 shows the vertical distribution of the wet bulk density over the upper 50 mm of the seabed.

Three distinct layers can be distinguished:

- biogenic gel-like layer of 1 to 5 mm thick uncosolidated mud (confirmed by diver observations) with wet bulk density of 850 to 1150 kg/m^3 (including local gasbubbles of maximum 1 mm diameter causing densities < 1000 kg/m^3);
- consolidating mud layer of 5 to 20 mm with wet bulk density of 1000 to 1150 kg/m^3;
- consoldated mud layer > 20 mm with wet bulk density of 1150 to 1300 kg/m^3.

The wet bulk density is lowest in the most quiescent regions of the inner cove.
The critical bed-shear stress for erosion was found to be in the range of 0.05 to 0.15 N/m^2. The critical stress increases with increasing chlorophyll content. The chlorophyll content was higher in shallower depths with higher light intensity.

Bed type	Percentage mud (<63 μm)	Mean size d_{50} (μm)	Dry bulk density (kg/m^3)	Chlorophyll content (μg/ml≅μg/g)	Critical shear stress for surface eosion (N/m^2)
Subtidal channel bed, Nova Scotia, Upper South Cove, Lunenburg Bay, Canada	20%-30%	30-40	< 400	< 5	0.05-0.15

Table 3.5 *Critical bed-shear for erosion at subtidal channel bed, Lunenburg Bay, Nova Scotia, Canada*

Figure 3.8 shows critical bed-shear stress as function of wet bulk density from six seabed stability studies using the sea carousel in widely varying environments. The erosion thresholds reported for pure mud of Inner Cove region (Nova Scotia) lie at the lower end of wet bulk density values. Although the sediment chlorophyll and carbohydrate contents lead to somewhat higher critical stresses, the low bulk density values may be responsible for the generally low erosion thresholds.

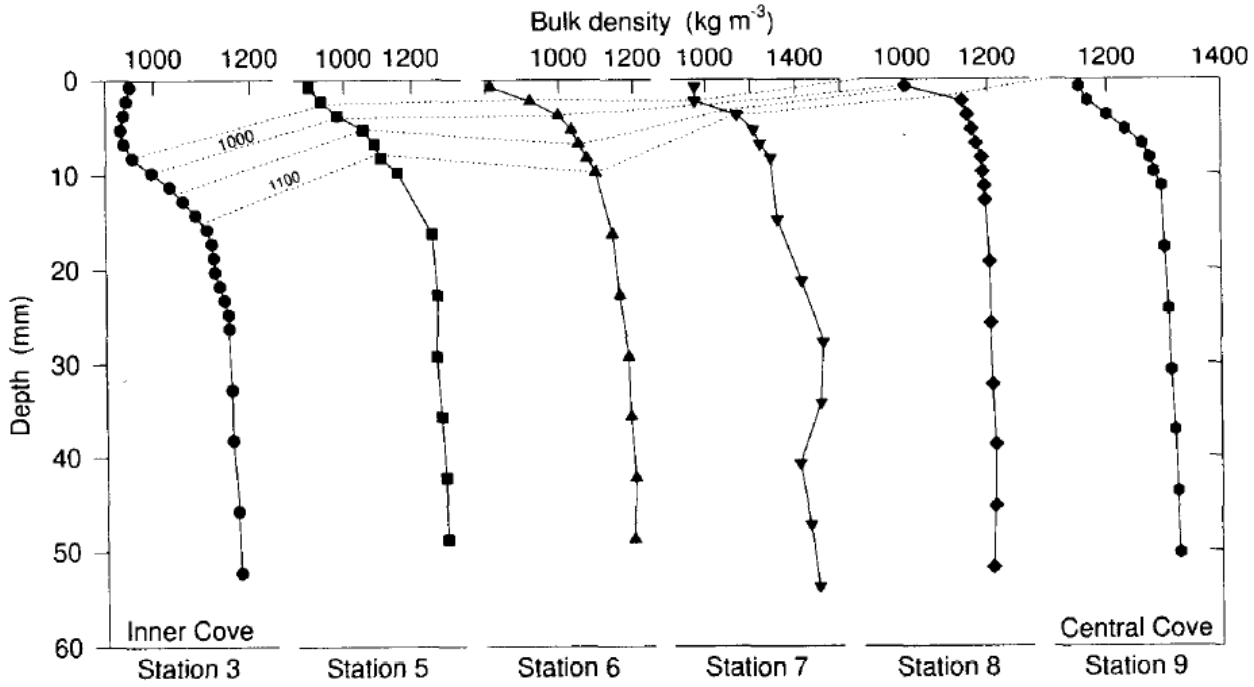

Figure 3.7 *Wet bulk density profiles at stations in water depths between 3 and 8 m, Inner cove, Canada*

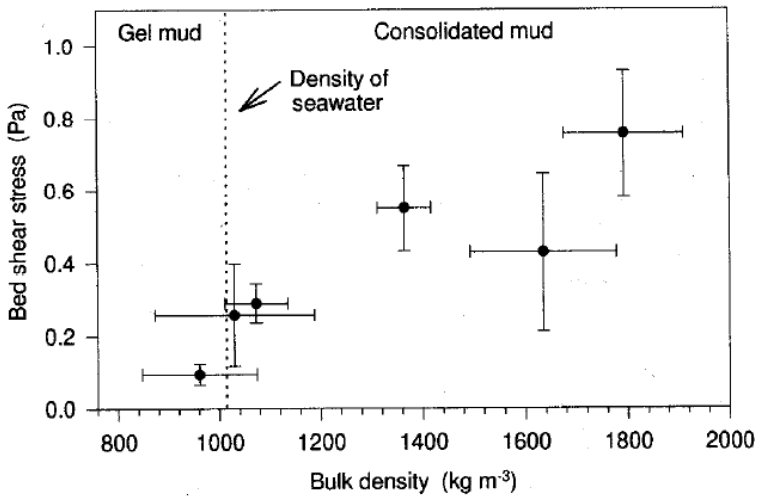

Figure 3.8 *Relationship between critical bed-shear stress and bulk density; six different locations (Manitounuk Sound, Humber Estuary, Miramichi Bay, Hamilton Harbour, Fraser River, Lunenburg Bay)*

4. References

Amos, C.L., Daborn, G.R., Christian, H.A., Atkinson, A. and Robertson, A., 1992. In situ erosion measurements on fine-grained sediments from the Bay of Fundy. Marine geology, Vol. 108, 175-196

Amos, C.L., Sutherland, T.F. and Zevenhuizen, J., 1996. The stability of sublittoral, fine-grained sediments in a subarctic estuary. Sedimentaology Vol. 43, 1-19

Amos, C.L., Feeney, T., Sutherland, T.F. and Luternauer, J.L., 1997. The stability of fine-grained sediments from the Fraser River Delta. Estuarine, Coastal and Shelf Science, Vol. 45, 507-524

Andersen, T.J., 2001. Seasonal variation in erodibility of two temperate microtidal mudflats. Estuarine, coastal and Shelf Science, Vol. 53,1-12

Andersen, T.J.Lanaru, M., Van Bernem, C., Pejrup, M. and Riethmueller, R., 2010. Erodibility of a mixed mudflat dominated by microphytobenthos and Cerastoderma edule, East Frisian Wadden Sea, Germany. Estuarine, Coastal and Shelf Science, Vol. 87, 197-206

Barry, K.M., Thieke, R.J. and Mehta, A.J., 2006. Quasi-hydrodynamic lubrication effect on clay particles on sand grain erosion. Estuarine, Coastal and Shelf research, Vol. 67, p. 161-169.

Bauamt fur Kustenschutz, Norden, 1987. Tiefenstabilisierung von Aussentiefs mit Naturuntersuchungen am Nessmersieler Aussentief.

Bisschop, R., 2018. Erosion of sand at high velocities; an experimental study. Doctoral Thesis, Department of Civil Engineering, Delft University of Technology, Delft, The Netherlands.

Delft Hydraulics, 1989. NOGAT Offshore Pipeline; report on erodibility tests. Report H1050, Delft, The Netherlands

Deltares 2016. KPP Navigation channel Holwerd; analysis of dredging data, bottom soundings and bottom composition. Report No. 1230378 (in Dutch), Delft, The Netherlands

Dey, S. 2003. Incipient motion of bivalve shells on sand beds under flowing water. Journal of Hydraulic Engineering, 232-240

Dankers, P.J.T., 2006. On the hindered settling of suspensions of mud and mud-sand mixtures. Doctoral Thesis, Technical University of Delft, Delft, The Netherlands

Dou, Guoren, 2000. Incipient motion of sediment under currents. China Ocean Engineering, Vol. 14, No. 4, p. 391-406.

Egiazaroff, P.I., 1965. Calculation of non-uniform sediment concentrations. Journal of the Hydraulics Division, ASCE, Vol. 91, HY 4.

Govers, G., 1987. Initiation of motion in overland flow. Sedimentology, Vol. 34, 1157-1164

Houwing, E.J., 2000. Sediment dynamics in the pioneer zone in the land reclamation area of the Waddenzee, Groningen, The Netherlands. Doctoral Thesis, Department of Physical Geography, University of Utrecht, Utrecht, The Netherlands.

HR Wallingford, 1992. Tidal transport of mud/sand mixtures. Report SR 257, Wallingford, UK

Jacobs, W., 2011. Sand-mud erosion from a soil mechanical perspective. Doctoral Thesis, Technical University of Delft, Department of Civil Engineering, Delft, The Netherlands

Kamphuis, J. W. and Hall, K.R., 1983. Cohesive material erosion by unidirectional current, Journal of Hydraulic Engineering, Vol. 109, 39– 62.

Kothyari, U.C. and Jain, R.K., 2008. Influence of cohesion on the incipient motion condition of sediment mixtures. Water Resources Research, Vol. 44, W04410, doi:10.1029/2007WR006326.

Laflen, J. M., and Beasley, R.P., 1960. Effect of compaction on critical tractive forces in cohesive soils, Res. Bull. 749, Agric. Exp. Stat. Univ. of Missouri, USA.

Le Hir, P., Cann, P., Waeles, B., Jestin, H., and Bassoullet, P., 2008. Erodibility of natural sediments: experiments on sand/mud mixtures from laboratory and field erosion tests. Sediment and Ecohydraulics, Intercoh 2005, Saga, Japan. Proceedings in Marine Science, Vol. 9. Edited by Kusuda, T., Yamanishi, H., Spearman, J. and Gailani, J.Z.

Li, J., Wan, X., He, Q., Ying, M., Shi, L.-Q., and Hutchinson, S. M., 2004. "In-situ observation of fluid mud in the North passage of Yangtze Estuary, China." China Ocean Eng., 18(1), 149–156.
Lick, W., Jin, L. and Gailani, J., 2004. Initiation of movement of quartz particles. Journal of Hydraulic Engineering, ASCE, Vol. 130, No.8, 755-761.
Lim, S.S., 2006. Experimental investigation of erosion in variably saturated clay soils. Doctoral Thesis, School of Civil and Environmental Engineering, University of New South Wales, Australia
Loiseleux, T., Grondet, P., Rabaud, M. and Doppler, D. 2005. Onset of erosion and avanlanche for an inclined granular bed sheared by a continuous laminar flow. Physics of Fluid 17, 103304
Long, M. and Menkiti, C.O., 2007. Geotechnical properties of Dublin boulder clay. Géotechnique Vol. 57, No. 6, 595-611. Doi: 10.1680/geot.2007.57.7.595
LVRS-Consultancy, 2019. Erosional behaviour of Boom Clay. www.leovanrijn-sediment.com
Mantz, P.A., 1977. Incipient transport of fine grains and flakes by fluids-extended Shields diagram. Journal of Hydraulics Division, ASCE, Vol. 103, HY8
Miedema, S.A. and Ramsdell, R.C., 2011. Hydraulic transport of sand/shell mixtures in relation with the critical velocity. Terra et Aqua, Vol. 122, 18-27
Miller, M.C., McCave, I.N. and Komar, P.D., 1977. Threshold of sediment motion under unidirectional current. Sedimentology, Vol. 24, 507-527
Mitchener, H. and Torfs, H., 1996. Erosion of mud/sand mixtures. Coastal Engineering, Vol. 29,, p. 1-25.
Mostafa, T.S. and Imran, J., 2008. Erosion resistance of cohesive soils. Journal of Hydraulic Research, Vol. 46, No. 6, 777-787
Mobley, J., Melville, J. and Parker, F., 2009. Evaluation of scour potential of cohesive soils. Report 930-644. Highway Research Center, Auburn University, Alabama, USA
Mostafa, T.S., Imran, J., Chaudhry, M.H. and Kahn, I.B., 2008. Erosion resistance of cohesive soils. Journal of Hydraulic Research, Vol. 46, No. 6, 777-787
Opera 2015. Properties and behavior of the Boom Clay. Vlissingen, The Netherlands (www.covra.nl)
Panagiotopoulos, I., Sylaios, G. and Collins, M.B., 1994. Threshold studies of gravel size particles under the co-linear combined action of waves and currents. Sedimentology, Vol. 41, 951-963.
Pilotti, M. and Menduni, G., 2001. Beginning of sediment transport of incoherent grains in shallow shear flows. Journal of Hydraulic Research, Vol. 39, No. 2, 115-124.
Rijkswaterstaat 1996. Clay for dikes. TAW Technical Report. Department DWW, Delft, The Netherlands
Rijkswaterstaat/RIKZ 2002. Evaluation of the effects of the dispersal of Boom Clay in the Western Scheldt (in Dutch). Report 2002.052, Rijksinstituut voor Kust en Zee, The Hague, The Netherlands
Roberts, J., Jepsen, R., Gotthard, D. and Lick, W., 1998. Effects of particle size and bulk density on erosion of quartz particles. Journal of Hydraulic Engineering, ASCE, Vol. 124, No. 12.
Shields, A. 1936. Anwendung der ähnlichkeitsmechanik und der turbulenz forschung auf die geschiebebewegung. Mitt. der Pruess. Versuchsamst. für Wasserbau und Schiffbau. Heft 26, Berlin, Germany
Smerdon, E.T. and Beasley, R.P., 1961. Critical tractive forces in cohesive soils. Agricultural Engineering, St. Joseph, Mich., 42(1), 26–29.
Sutherland, T.F., Amos, C.L. and Grant, J., 1998. The effect of buoyant biofilms on the erodibility of sublittoral sediments of a temperate microtidal estuary. Limnology Oceanography Vol. 43, No. 2, 225-235
Thorn, M.F.C., 1981. Physical processes of siltation in tidal channels. Proc. Hydraulic Modelling, Paper No. 6, ICE, London, UK.
Tolhurst, T.J., Riethmueller, R. and Paterson, D.M., 2000. In-situ versus laboratory analysis of sediment stability from intertidal mudflats. Continental Shelf Research, Vol. 20, 1317-1334
Van, L.A., Villaret, C., Pham Van Bang, D. and Schuettrumpf, H., 2012. Erosion and deposition of the Gironde mud. ICSE 6, Paris
Van Rijn, L.C., 1991, 2011. Principles of fluid flow and surface waves in rivers, estuaries and coastal seas. www.aquapublications.nl

Van Rijn, L.C., 1993, 2006. Principles of sediment transport in rivers, estuaries and coastal seas. www.aquapublications.nl
Van Rijn, L.C., 2005, 2015. Principles of sedimentation and erosion engineering in rivers, estuaries and coastal seas. www.aquapublications.nl
Van Rijn, L.C., 2020. Erodibility of mud-sand bed mixtures. Journal of Hydraulic Engineering, Vol. 146(1): 04019050, ASCE, USA
Van Rijn, L.C., Bisschop, R. and Van Rhee, C. 2019. Modified Sediment pick-up function. Journal of Hydraulic Engineering ASCE, Vol. 145(1). DOI: 10.1061/(ASCE)HY.1943-7900.0001549
Vinzon, S.B. and Mehta, A.J., 2003. Lutoclines in high concentration estuaries: some observations at the Mouth of the Amazon, p. 243-253. Journal of Coastal Research, Vol. 19, No. 2
Ward, B.B., 1967. Surface shear and incipient motion of uniform grains. Doctoral Thesis, University of Arizona, USA
White, C.M., 1940. The equilibrium of grains on the bed of a stream. Proceedings of Royal Society of London, Series A, No. 958, Vol. 174, 332-338
White, S.J., 1970. Plane bed thresholds of movement of fine grained sediments. Nature, Vol. 228, 152-153
Winterwerp, J.C., 1999. On the dynamics of high-concentrated mud suspensions. Doc. Thesis. Dep. of Civil engineering, Delft University of Technology, Delft, The Netherlands
Winterwerp, J.C., 2001. Stratification effects by cohesive and noncohesive sediment. Journal of Geophysical Research, Vol. 106, No. C10. p. 22559-22574
Winterwerp, J.C., Van Kesteren, W.G.M., Van prooijen, B. and Jacobs, W., 2012. A conceptual framework for shear flow-induced erosion of soft cohesive sediment beds. Journal of Geophysical Research, Vol. 117, C10020,
Wolters, G., Nieuwenhuis, J.W., Van der Meer, J. and Klein Breteler, M., 2008. Large scale tests of boulder clay erosion at the Wieringermeer dike (IJsselmeer). ICCE 2008, Hamburg, Germany
Wu, W., Perera, C., Smith, J. and Sanchez, A., 2017. Critical shear stress for erosion of sand and mud mixtures. Journal of Hydraulic Research, Doi.org/10.1080/00221686.2017.1300195
Yalin, M.S. and Karahan, E., 1979. Inception of sediment transport. Journal of Hydraulics Division, ASCE, Vol. 105, No. Hy 11, 1433-1443
Zanke, U.C.E., 2003. On the influence of turbulence on the initiation of motion. International Journal of Sediment Research, Vol. 18, No. 1, 17-31.